

Measuring the Earth's Magnetic Field from Space: Concepts of Past, Present and Future Missions

N. Olsen · G. Hulot · T.J. Sabaka

Received: 13 June 2010 / Accepted: 6 July 2010 / Published online: 7 August 2010
© Springer Science+Business Media B.V. 2010

Abstract Observations of the Earth's magnetic field from low-Earth orbiting (LEO) satellites started very early on, more than 50 years ago. Continuous such observations, relying on more advanced technology and mission concepts, have however only been available since 1999. The unprecedented time-space coverage of this recent data set opened revolutionary new possibilities for monitoring, understanding and exploring the Earth's magnetic field. In the near future, the three-satellite *Swarm* constellation concept to be launched by ESA, will not only ensure continuity of such measurements, but also provide enhanced possibilities to improve on our ability to characterize and understand the many sources that produce this field. In the present paper we review and discuss the advantages and drawbacks of the various LEO space magnetometry concepts that have been used so far, and report on the motivations that led to the latest *Swarm* constellation concept. We conclude with some considerations about future concepts that could possibly be implemented to ensure the much needed continuity of LEO space magnetometry, possibly with enhanced scientific return, by the time the *Swarm* mission ends.

Keywords Low earth-orbiting satellites · Magnetic field modeling · *POGO* · *Magsat* · *Ørsted* · *SAC-C* · *ST-5* · *CHAMP* · *Swarm*

1 Introduction

Prior to the satellite era, only ground-based magnetic observations were available for modeling the Earth's magnetic field, and this was a serious limitation because of the finite number

N. Olsen (✉)
DTU Space, Technical University of Denmark, Juliane Maries Vej 30, 2100 Copenhagen, Denmark
e-mail: nio@space.dtu.dk

G. Hulot
Equipe de Géomagnétisme, Institut de Physique du Globe de Paris, Université Paris Diderot,
INSU/CNRS, 4, Place Jussieu, 75252 Paris cedex 05, France

T.J. Sabaka
Geodynamics Branch, NASA GSFC, Greenbelt, MD, USA

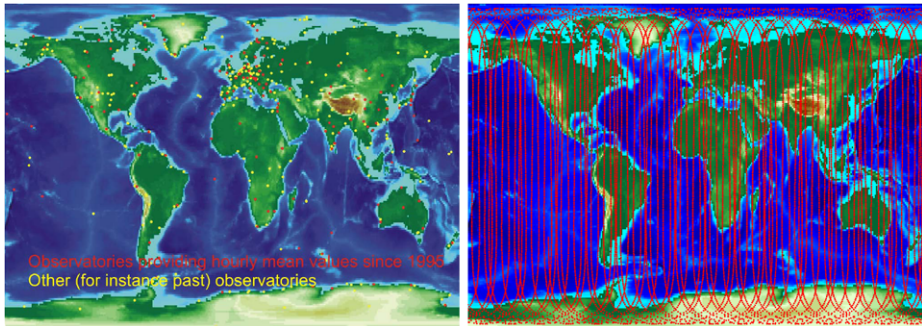


Fig. 1 Distribution of present ground observatory network (*left*) and ground-track of 3 days satellite data (*right*)

of permanent magnetic observatories (Fig. 1 left). As Low-Earth-Orbiting (LEO) satellites can quickly provide a much better geographical coverage than ground observatories (Fig. 1 right), the community was therefore quick to realize that magnetic measurements from space could be made at good use to overcome this limitation. Indeed measurements of the Earth's magnetic field from space began very early on, some 50 years ago, with the launch of the *Sputnik 3* satellite in 1958 (Dolginov et al. 1962). But for various technical reasons, these early measurements were of low resolution and only provided regional coverage. Truly global geographical coverage, which is essential for determining global models of the geomagnetic field, was first achieved by the *POGO* satellite series that measured the magnetic field intensity between 1965 and 1971 (Cain 2007). Unfortunately it was soon realized that such intensity measurements did not provide enough information to recover robust global models of the geomagnetic field (Backus 1970). Properly oriented vector measurements are required. This much more challenging task was first achieved in 1979–80 by the *Magsat* satellite, with considerable success (Purucker 2007). More recently, the launch of *Ørsted* in February 1999 (Neubert et al. 2001; Olsen 2007), *CHAMP* in July 2000 (Reigber et al. 2002; Maus 2007a) and *SAC-C* in November 2000, opened revolutionary new possibilities, by providing a continuous stream of high quality (and mainly vectorial) data ever since, leading to many further scientific achievements. It is expected that even more achievements will soon be made, thanks to the ESA *Swarm* mission, consisting of three satellites to be launched in 2012 into an innovative constellation (Friis-Christensen et al. 2006, 2009).

But even with the help of such satellites, the challenge of recovering high-precision global models of the geomagnetic field remains formidable. The main reason for this is that the magnetic field measured locally in an observatory or on board a satellite is the result of the superposition of fields produced by many different sources, with overlapping spatial and temporal scales (Fig. 2). The main source lies within the core, where the so-called “geodynamo” operates. At the Earth's surface and above, it produces a field which is dominantly dipolar. But this so-called “core field” also involves many other spatial scales, of decreasing magnitude as smaller scales are considered. It evolves on secular to decadal time scales, its shortest time scales (of less than typically a year) being screened by the slightly electrically conducting mantle that it must permeate to reach the Earth's surface. This field is not the only one produced within the solid Earth. Magnetized rocks indeed lie within the lithosphere (where the temperature is low enough for significant magnetization to be found). The distribution of this magnetization (both remanent and induced by the core field) is the complex result of the tectonic history of the lithosphere, and this produces a field with

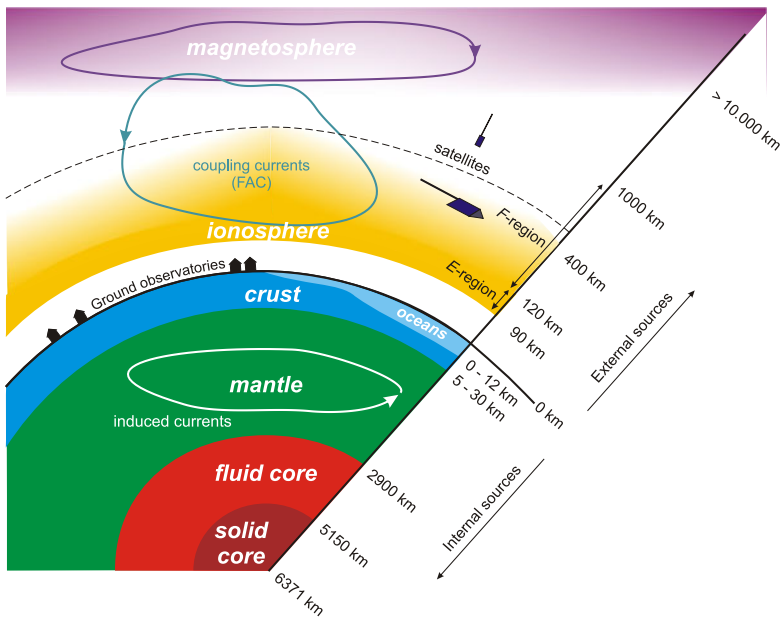


Fig. 2 Sketch of the various sources contributing to the near-Earth magnetic field

roughly comparable magnitudes at all geological spatial scales. At or close to the surface, this so-called “lithospheric field” is weaker than the core field when large scales are considered, but ultimately dominates the field of internal origin when smaller scales (typically less than a few thousand of kilometers) are considered. It too changes with time, but so weakly that these changes cannot yet be detected (except very locally, when new volcanic rocks settle, for instance). Weak magnetic field sources can also be found in the oceans as a result of the movement of the electrically conducting water in the core field. Other very significant sources are to be found starting at altitude 100 km above the Earth’s surface. These produce the so-called field of external origin, and are to be found in the form of electrical currents coupling and flowing within the ionosphere and the magnetosphere. The corresponding fields involve both very large (planetary, especially for the magnetospheric field), and much smaller (local) spatial scales. It has some slowly changing components (for instance those related to the 11-year solar cycle), but mainly changes on much shorter time scales (typically days and less) than the field of internal origin. Finally, these fields also induce weak, but significant, electrical currents within the solid Earth, which in turn produce some so-called externally induced internal fields. A more detailed account of these various sources can be found in e.g. Olsen et al. (2010b), and recent reviews providing even more information about the fields produced can be found in e.g. Hulot et al. (2007), Jackson and Finlay (2007), Hulot et al. (2010), Finlay et al. (2010) for the core field, Purucker and Whaler (2007), Thébault et al. (2010) for the lithospheric field, Manoj et al. (2006), Maus (2007b), Kuvshinov (2008) for the field produced within the oceans, Kivelson and Russell (1995), Kelley (2009) for the field of external origin, and Constable (2007), Kuvshinov (2008) for externally induced internal fields.

As a consequence of this multiplicity of sources and magnetic fields, a number of specific issues have to be taken into account which still somewhat limit the advantage of measuring the magnetic field from space. Using LEO satellite data is indeed not technically as simple

as using observatory data. First, whereas observatories are at fixed locations, so that any changes observed in magnetic observatories can unambiguously be associated with time changes in the observed magnetic field, satellites keep on moving, with a velocity of typically 8 km/s at an altitude of 400 km, so that changes observed in the satellite data are the result of a combination of temporal and geographical changes in the field measured. This results in space-time-aliasing that needs to be disentangled. Second, whereas observatories measure the field in an essentially source free region (the electrically non-conductive atmosphere), satellites orbit in regions of the ionosphere where local electrical currents are to be found (recall Fig. 2). This requires a different way of mathematically representing the field and introduces additional issues. Finally, measuring the magnetic field from an altitude of a few hundred kilometers, as is the case with LEO satellites, corresponds roughly to averaging the field produced by internal sources over an area of this dimension, thereby reducing the sensitivity of satellite data to the field produced by lithospheric sources with spatial scales of less than a few hundred kilometers.

Various near-Earth environment space magnetometry concepts have nevertheless been developed to overcome these limitations over the past decades, with the main (but not only) goal of improving our ability to recover the field of internal origin (i.e. the core and lithospheric fields). In the present paper, we will provide a general overview of the way these concepts have evolved since the early days of the *POGO* satellite series, progressively leading to the latest concept proposed for the ESA *Swarm* satellite constellation soon to be launched. Describing all aspects of this evolution is however not within reach of such a necessarily limited review. In particular, most of the methodological progress that has been made in parallel to the introduction of new satellite concepts will not be described in detail. Reports on these progress and currently developing methodologies can be found in many books and reviews, such as e.g. Langel (1987), Langel and Hinze (1998), Sabaka et al. (2004, 2010), Sabaka and Olsen (2006), Hulot et al. (2007, 2010), Thébault et al. (2010), Gillet et al. (2010), Olsen et al. (2010a). Also, even though these progress have led to some improvement in the recovery of the field of external origin, the identification of local sources at LEO satellite altitude (e.g. Lühr et al. 2002; Maus and Lühr 2006; Stolle et al. 2006; Sabaka and Olsen 2006), as well as in the investigation of externally induced fields from space (e.g. Kuvshinov and Olsen 2006; Kuvshinov 2008), those aspects will not be discussed in any detail, as much of the evolution in the near-Earth environment space magnetometry concepts has mainly be driven by considerations on the improvement of the recovery of the field of internal origin.

To illustrate this evolution and the motivations that drove it, we will therefore mainly rely on fairly simple LEO mission simulations, ignoring all external, oceanic and externally induced internal sources, and even ignoring the fact that the field of internal origin is slowly time-varying. This will allow us to rely on a simple first order method to assess the relative performances of various satellite concepts with respect to the recovery of the field of internal origin (Sect. 2). This method will be applied to various near-Earth environment space magnetometry concepts (Sects. 3 and 4), successful examples of which will also be briefly presented (Sect. 5). Those assumptions are extremely simplifying, and as described in the above-mentioned references, actual field modeling strategies have of course accounted for what will be ignored here. These aspects will nevertheless briefly be mentioned whenever necessary. This will be the case in particular when we will report on the much more elaborate simulations that have been carried out in the course of the preparation of the *Swarm* satellite constellation mission (Sect. 6). Finally, ideas and concepts for satellite missions after *Swarm* will be briefly mentioned in Sect. 7. A “timeline” presenting the various satellite missions that are of relevance for modeling the Earth’s magnetic field is presented in Fig. 3.

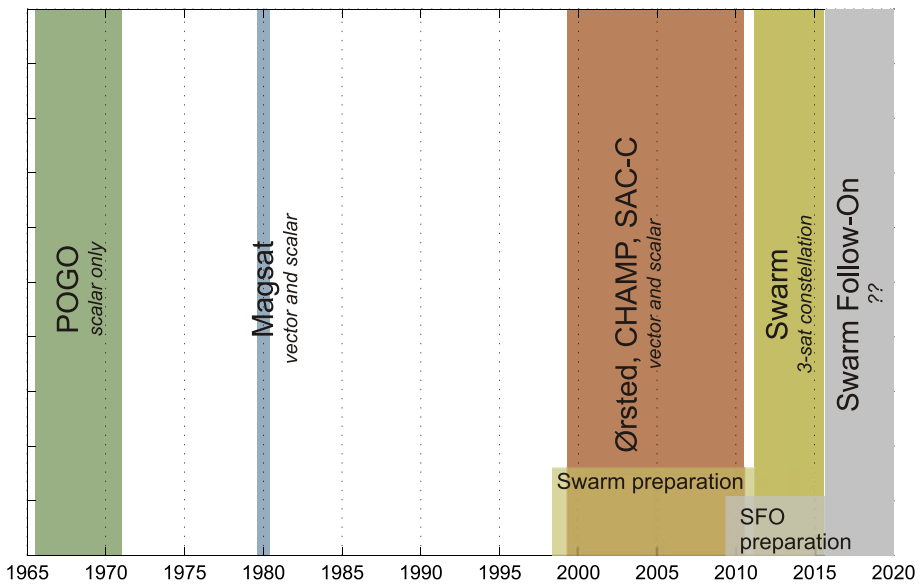


Fig. 3 Timeline of the various high-precision satellite missions

2 Assessing the Relative Performances of Satellite Concepts

In regions without any sources, such as the neutral atmosphere, the magnetic field $\mathbf{B} = -\nabla V$ can be expressed as the negative gradient of a scalar potential V which solves the Laplace equation $\nabla^2 V = 0$.

Expanding V in a series of spherical harmonics leads to

$$\begin{aligned}
 V &= V^{\text{int}} + V^{\text{ext}} \\
 &= a \sum_{n=1}^{N_{\text{int}}} \sum_{m=0}^n (g_n^m \cos m\phi + h_n^m \sin m\phi) \left(\frac{a}{r}\right)^{n+1} P_n^m(\cos\theta) \quad (1a)
 \end{aligned}$$

$$\begin{aligned}
 &+ a \sum_{n=1}^{N_{\text{ext}}} \sum_{m=0}^n (q_n^m \cos m\phi + s_n^m \sin m\phi) \left(\frac{r}{a}\right)^n P_n^m(\cos\theta) \quad (1b)
 \end{aligned}$$

(Chapman and Bartels 1940; Langel 1987), where r, θ, ϕ are geocentric spherical coordinates, a is a reference radius (typically Earth's mean radius $a = 6371.2$ km is used), P_n^m are the associated Schmidt semi-normalized Legendre functions, N_{int} is the maximum degree and order of the internal potential coefficients g_n^m, h_n^m , and N_{ext} is that of the external potential coefficients q_n^m, s_n^m . These coefficients are known as the Gauss coefficients.

Modeling the geomagnetic field from ground data then consists in recovering estimates of the Gauss coefficients from the data. The set of recovered g_n^m, h_n^m Gauss coefficients defines a model of the field of internal origin, while the set of recovered q_n^m, s_n^m Gauss coefficients defines a model of the field of external origin. To account for the fact that both fields vary in time, various temporal representations of these coefficients can of course be used.

One very important property of this mathematical representation of the geomagnetic field is that in principle, provided perfect vector measurements can be made everywhere at the

Earth's surface at each given moment, all Gauss coefficients can be recovered in a unique way. Also, once those coefficients have been recovered, they may next be used to compute the field of internal origin anywhere above, and the field of external origin everywhere below, where their respective sources lie (see e.g. Sabaka et al. (2010) where most of the mathematical representations and theorems we will rely on or mention in the course of this paper, can be found). Unfortunately, because of the limited number of observatories available at the Earth's surface (recall Fig. 1 left), only the largest scales of these fields (i.e. the Gauss coefficients with order m and degree n lower than, say, 8) can be recovered from observatory data. Hence the potential benefit of relying on the much denser geographical coverage provided by LEO satellites.

However, analyzing magnetic data from LEO satellites requires some care, in particular because they do not orbit in the neutral atmosphere, but in the F -region of the ionosphere (recall Fig. 2). Some of the ionospheric field with sources in the E -region, of external origin from the point of view of observatories, are perceived as being of internal origin by LEO satellites. In addition, local currents to be found in the F -region can produce local "toroidal" fields that cannot be represented in terms of the formalism of (1). This is the case of so-called field-aligned currents (FAC), i.e. currents coupling the magnetosphere to the ionosphere and flowing along the direction of the field-lines of the ambient main magnetic field.

There are several ways one can deal with these complications (see e.g. Hulot et al. 2007; Sabaka et al. 2010 for details and additional references). One is to introduce a more elaborate mathematical description of the field produced at satellite locations, which can be related to the mathematical description of the field produced at observatory locations (see (1)). This makes it possible to simultaneously model the field of internal origin, the E -region ionospheric field (seen as internal by the satellites, but as external by the ground observatories), the local toroidal field sensed by the satellites in the F -region, the magnetospheric field (seen as external by both satellites and observatories), and even the externally induced fields. This approach, known as the "Comprehensive Modeling" (CM) approach (see e.g. Sabaka et al. 2004) also makes it possible to take the temporal variations of the various fields into account, despite the fact that the satellites keep on moving.

An alternative approach, often taken for the purpose of specifically recovering the field of internal origin, is to rely on the selection of satellite data least affected by the field of external origin (such as at night time, when ionospheric currents are weakest), and model the field with the help of (1), where only a few unavoidable external field terms are kept to describe the ever present large-scale magnetospheric field. As field-aligned currents are also always present at high (auroral) latitudes, but happen to much less affect the intensity than the full vector satellite data, this approach also usually involves only using intensity data at high (magnetic) latitude (for one of the simplest example of such an approach, see e.g. Olsen et al. 2000).

In what follows, and for the purpose of illustrating the relative performance of the various satellite concepts, it is mainly simulations inspired by this second type of approach that we will rely on. Only in the case of the more elaborate discussion of the *Swarm* mission in Sect. 6, will we present simulations based on a CM type of approach.

To assess the performance of the different satellite orbit configurations, we thus synthesize satellite positions for circular orbits of a certain inclination i (where $i = 90^\circ$ corresponds to an exactly polar orbiting satellite, i.e. an orbit that crosses the geographic poles). For each case, 10,000 satellite positions are synthesized, which corresponds to one week worth of continuous satellite data of 1 min sampling rate (a typical value in field modeling), or to two weeks of data if only one half of each orbit (for instance the night-side part) are taken. We assume that the observations only contain internal field contributions (i.e. that external

field contributions either have been corrected for or are absent because only certain selected data are used) and is static (which is perfectly legitimate when considering only one or two weeks of data).

The goal of field modeling is then to estimate the Gauss coefficients g_n^m, h_n^m of internal origin (see (1)) from magnetic field observations, which can either be the components of the field vector or magnetic field intensity. For this purpose we collect the unknown Gauss coefficients (model parameters) g_n^m, h_n^m in the model vector \mathbf{m} and the data (which may comprise of vector and/or scalar intensity observations) in the data vector \mathbf{d} . In the case of vector data alone, there is a linear relationship between observations \mathbf{d} and model unknowns \mathbf{m} :

$$\mathbf{d} = \mathbf{G}\mathbf{m} \tag{2}$$

with \mathbf{G} as the data kernel matrix. Assuming identical data errors (variance σ_d^2), the model vector \mathbf{m} can be determined as the least-squares solution

$$\mathbf{m} = (\mathbf{G}^T \mathbf{G})^{-1} \mathbf{G}^T \mathbf{d} \tag{3}$$

and the covariance matrix of the model parameters is given by

$$\mathbf{C} = \sigma_d^2 (\mathbf{G}^T \mathbf{G})^{-1}. \tag{4}$$

The diagonal elements of \mathbf{C} are the variances σ_g^2 of the estimated Gauss coefficients g_n^m, h_n^m .

Note that in this linear case (and for assumed equal data errors) the model covariance matrix \mathbf{C} is independent on the actual magnetic field measurements \mathbf{d} ; its computation only requires knowledge on the satellite positions (and the type of measurements, for instance which vector field components are measured). Maps of σ_g^2 in dependence on spherical harmonic degree n and order m of the Gauss coefficient therefore only depend on the geometry of the orbit. They can thus be used to investigate how well, in relative terms, the internal magnetic field can be determined from a given satellite configuration, independently of the exact performance of the instruments on board the satellites.

If measurements of the magnetic field intensity are also (or only) used for field modeling, a situation we will also consider, the relationship between data vector \mathbf{d} and model unknowns \mathbf{m} becomes non-linear:

$$\mathbf{d} = \mathcal{G}(\mathbf{m}), \tag{5}$$

and the situation is slightly different.

But we may then rely on the standard strategy used to solve this equation, which is based on a linearization using a starting model \mathbf{m}_0 . The resulting equations are similar to (2) to (4), except that the data kernel matrix \mathbf{G} now depends on the model \mathbf{m} , and (3) has to be solved iteratively. As a result, the model covariance matrix \mathbf{C} , equation (4), then also depends on the geometry of the magnetic field. But since the Earth's magnetic field at or above the surface is dominated by the dipole field, choosing the first terms of a spherical harmonic expansion of the present field as starting (background) model \mathbf{m}_0 , is sufficient to recover a reasonably realistic estimate of the covariance matrix \mathbf{C} corresponding to a given satellite configuration. The simulations described below have been performed using the OIFM field model (Olsen et al. 2000) up to degree and order 13 as such a starting model. A map of the radial component B_r predicted by this model at the Earth's surface is shown in Fig. 4.

In what follows, we will rely on such covariance matrix calculations to illustrate the relative merits of the various satellite concepts we investigated.

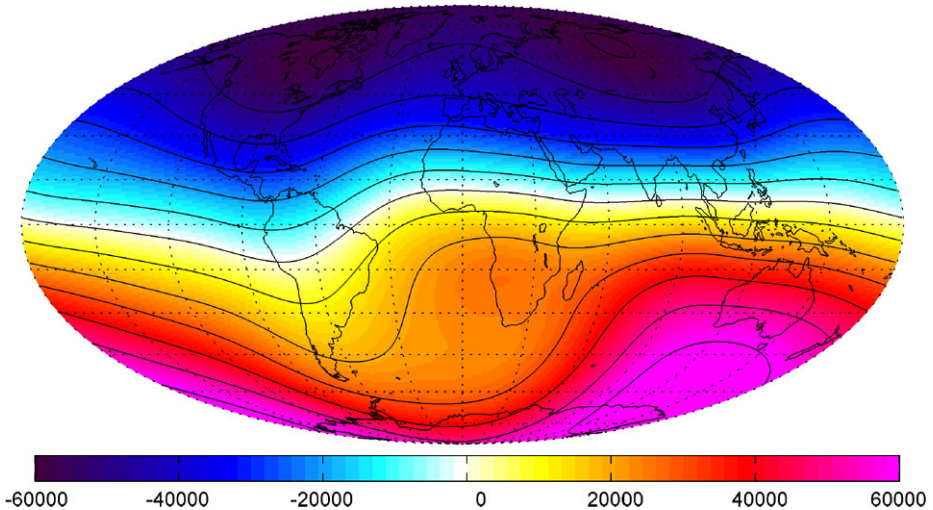


Fig. 4 B_r (in nT) predicted by the OIFM model (Olsen et al. 2000) up to degree and order 13 at the Earth's surface for epoch 2000.0. Contour interval is 10,000 nT

3 Single Satellite Concepts

We first consider the simple case of 10,000 magnetic vector measurements taken at all latitudes by a satellite in a circular polar orbit (inclination $i = 90^\circ$) at altitude 450 km.

For this case, Fig. 5a shows the dependence of σ_g^2 on spherical harmonic degree n and order m (we only present coefficients up to $n = 40$), with $m \geq 0$ referring to the coefficients g_n^m and $m < 0$ referring to h_n^m . Since the *absolute* value of σ_g^2 is proportional to the data variance σ_d^2 we discard this dependence and present the *relative* value of σ_g^2 on an arbitrary scale which, however, is the same for all the cases presented in Fig. 5.

Under the (highly idealistic) conditions described above, a very good recovery of the Gauss coefficients is clearly possible. Best resolved are the low-degree coefficients. There is a slight degradation towards higher degrees, which is expected: In the case of an equal-area distribution of data an approximate analytic solution exists (Langel 1987, eq. (124)) with variances σ_g^2 of the obtained Gauss coefficients proportional to $(n + 1)^{-1}$. This explains the increase of the variance with degree n that is obvious from Fig. 5a.

We now turn to a more realistic scenario. As already noted, the first satellites to extensively map Earth's magnetic field only measured the magnetic field intensity. Unfortunately, and as first explicitly demonstrated by Backus (1970) (see also Alberto et al. 2004; Sabaka et al. 2010), a unique determination of the magnetic field from just intensity measurements is not systematically guaranteed, even if such measurements are ideally assumed to be available at all locations (at one specific altitude). In practice however, when one relies on a finite number of intensity data and just searches for a finite number of Gauss coefficients, some practical uniqueness can be achieved, and the underlying fundamental non-uniqueness issue then translates into an extreme sensitivity of certain Gauss coefficients to any observational (or modeling) error. This effect, known as the *Backus effect* (or sometimes also the *perpendicular effect*, see e.g. Lowes 1975), particularly affects the sectorial coefficients g_n^n , h_n^n of the recovered field. This is well illustrated in Fig. 5b, which shows the σ_g^2 variances of the model covariance matrix \mathbf{C} in the case of a simulation based on 10,000 measurements at the same locations as in the previous case, but only for intensity values,

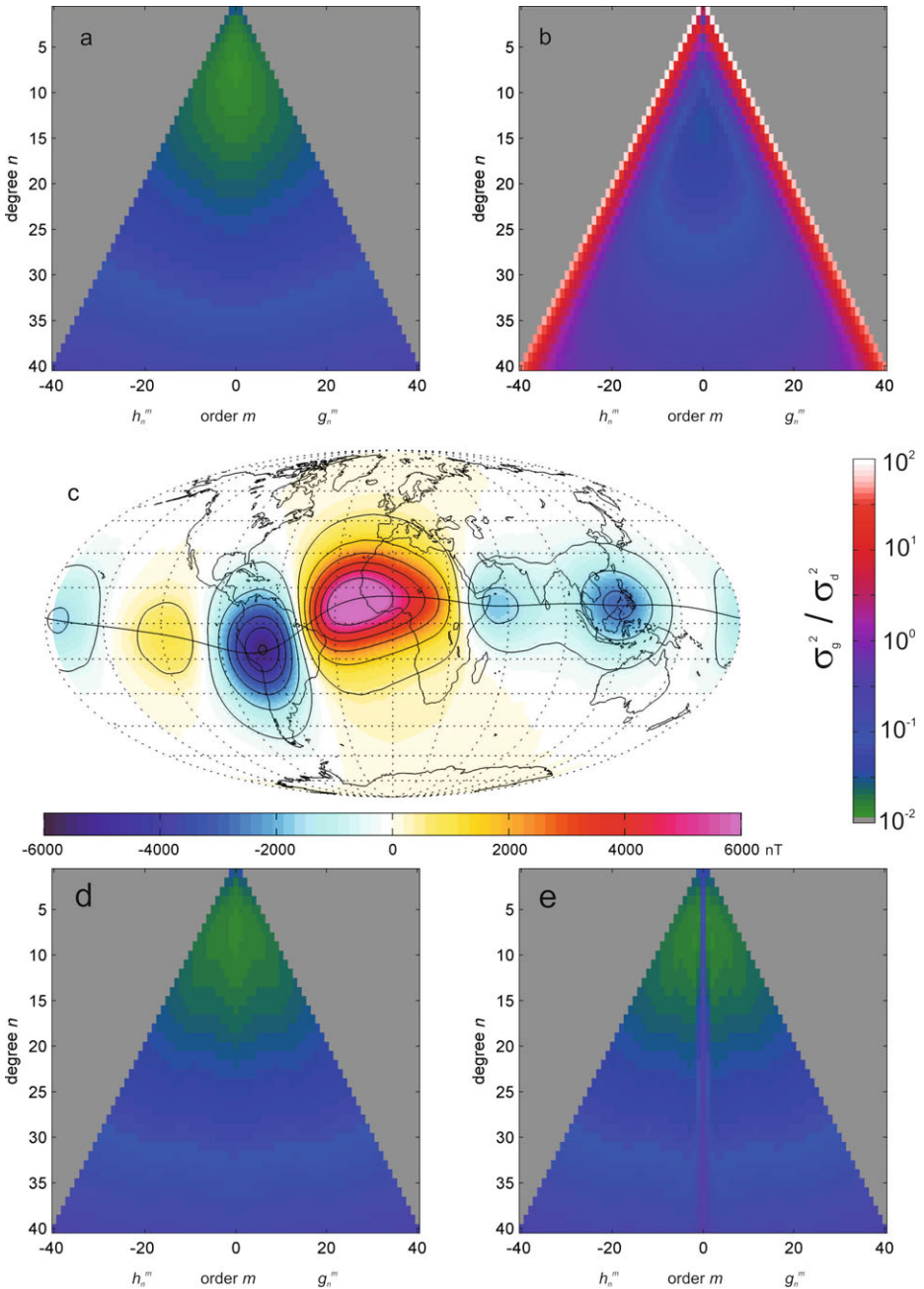


Fig. 5 (a): Variance of the recovered internal Gauss coefficients from 10,000 data points of the vector components obtained by a polar orbiting satellite at 450 km altitude. (b): Similar to (a) but using only magnetic field intensity data. (c): Difference in B_r at ground between original and recovered model when only magnetic intensity measurements are available (see text for details). (d): Similar to (a) but using only intensity data at latitudes poleward of $\pm 60^\circ$, else vector data. (e): Similar to (d) but for a satellite in a near-polar orbit of inclination $i = 97^\circ$

assuming the same arbitrary error on all measurements. The nuisance introduced by this *Backus effect* can also be illustrated by plotting the difference between a model computed from vectorial data and a model computed from intensity data taken at exactly the same locations (as was originally done by e.g. Stern et al. 1980), or by plotting the difference between the field produced by our starting model (the OIFM model up to degree 13, Fig. 4), and the field recovered from inverting the intensity measurements produced by this starting model at the 10,000 locations. Just inverting for a different number of Gauss coefficients (up to degree and order 50 in the present case) can lead to considerable differences, even in the case of noise-free data (Fig. 5c). The difference in the radial component of the field (B_r) at the Earth's surface can reach several thousands of nT, in large patches centered on the magnetic equator (where the field averages to typically 30,000 nT).

Finding ways of avoiding this Backus effect is intrinsically related to finding ways of removing the fundamental non-uniqueness problem associated with it. This can be achieved if in addition to knowing the field intensity, one knows something about the location of the magnetic equator (Khokhlov et al. 1997). Even approximate information can prove useful (Ultré-Guérard et al. 1998; Khokhlov et al. 1999), and this has led to some smart ways of minimizing the Backus effect, even when relying on intensity-only satellite data. Because these data can also be used to detect the local magnetic signature of the so-called Equatorial Electrojet (a narrow electrical current running along the magnetic equator in the E -region of the ionosphere), the location of this equator can indeed be pinpointed every time the satellite crosses the magnetic equator. As shown by Holme et al. (2005), localizing the magnetic equator in this way, and taking advantage of this additional information when inverting for a field model from just intensity data, can successfully remove much of the Backus effect. However, one should notice that knowledge of the position of the dip-equator only helps if there are no significant external (e.g. magnetospheric) field contributions. In addition, it should be stressed that relying on such a strategy is far less efficient than having directly access to full vector measurements, even with relatively low pointing accuracy (see e.g., Holme and Bloxham 1995, 1996).

Unfortunately full LEO satellite vector data cannot be taken advantage of as straightforwardly as we did to derive the results shown in Fig. 5a. As already noted, significant contributions from field-aligned currents are always to be found in the vector data measured at high auroral latitudes. Standard approaches based on data selection to recover the field of internal origin (as opposed to the more sophisticated CM approach), thus rely on scalar data, which are much less affected by those field-aligned currents, at latitudes polewards of, say, $\pm 60^\circ$ dipole latitude or so. Note that these latitudes are distant enough from the magnetic equator that the retained low latitude vector data implicitly provide the location of the magnetic equator, thus preventing the Backus effect from arising. Indeed a simulation that uses vector data at latitudes below $\pm 60^\circ$ but scalar data at higher latitude (Fig. 5d) nicely shows that the quality of the recovery is very similar to that of the ideal case when vector data are used at all latitudes (Fig. 5a).

All single satellite concepts considered in the above simulations assumed the satellite to be in an exact polar orbit (inclination $i = 90^\circ$). Achieving such an orbit is however very difficult and in practice all satellites have had orbits with an inclination different from 90° . This results in the satellites not covering a region around the geographic poles of half-angle $|90^\circ - i|$ (the *polar gap*). For the satellites that are commonly used in field modeling this angle varies between $|90^\circ - 87^\circ| = 3^\circ$ and $|90^\circ - 97^\circ| = 7^\circ$. Figure 5e shows the result of a simulation that is similar to the one presented in Fig. 5d but for a satellite with orbital inclination $i = 97^\circ$. Such an orbit clearly results in a degradation of the recovery of the near-zonal coefficients ($m \approx 0$). Since only spherical harmonics of order $m = 0$ contribute

to the magnetic field at the geographic poles, it is obvious that a lack of data near the poles results in poorer resolution of these coefficients. Note however that these coefficients can nevertheless be recovered as a result of the potential nature of the field of internal origin, which leads the data collected by the satellite at high latitudes to also have a contribution from sources within the polar gap.

4 Gradient Concepts

An obvious way to possibly improve on the performances of single-satellite mission concepts is to consider concepts based on two close-by orbiting LEO satellites. Such concepts would not only allow to double the amount of data collected during a given period of time, they would also make it possible to compute gradient estimates of field components, which can be expected to improve the retrieval of the high-degree coefficients of the field of internal origin. Such concepts have indeed been very successful in the case of gravity space missions, such as *GRACE* (Tapley et al. 2004) and *GOCE* (Drinkwater et al. 2003). Optimal spacecraft separation for deriving the gradients however depend on signal spectrum, instrument resolution, and on the smallest scales that should be resolved during the mission.

We first consider the potential benefit of making use of the East-West gradient of the magnetic field. For this purpose, we introduce the complex form of the spherical harmonic expansion of the field of internal origin,

$$V^{\text{int}} = a \sum_{n=1}^{N_{\text{int}}} \sum_{m=0}^n \left(\frac{a}{r}\right)^{n+1} \gamma_n^m P_n^m e^{im\phi}, \tag{6}$$

where $\gamma_n^m = g_n^m - ih_n^m$. The difference of the magnetic field vector measured by two satellites flying simultaneously with a longitudinal separation $\Delta\phi$ is then $\Delta\mathbf{B} = \mathbf{B}(r, \theta, \phi) - \mathbf{B}(r, \theta, \phi + \Delta\phi) = -\text{Re}\{\nabla \Delta V\}$, where ΔV is a spherical harmonic expansion with coefficients

$$\Delta\gamma_n^m = \gamma_n^m (1 - e^{im\Delta\phi}) \tag{7}$$

and $\text{Re}\{\cdot\}$ indicating that only the real part has to be taken (as done so far we again ignore the field of external origin). Hence by analyzing the difference of the magnetic field measured by two such satellites the Gauss coefficients γ_n^m are multiplied by some filter factors with filter gain $|(1 - e^{im\Delta\phi})| = \sqrt{2(1 - \cos m\Delta\phi)}$. For small values of $\Delta\phi$ this quantity becomes $|(1 - e^{im\Delta\phi})| \approx m\Delta\phi$, which indicates that knowledge of the East-West gradient of the magnetic field improves the determination of Gauss coefficients of high order.

Figure 6a shows the filter gain for three different values of longitudinal separation, $\Delta\phi$, of the satellites (both assumed to be on perfect circular polar orbits at 450 km altitude). If we for instance aim at recovering the field of internal origin up to spherical harmonics of degree and order 133 corresponding to a spatial scale of 300 km (the goal of the upcoming *Swarm* satellite constellation, see Sect. 6), the optimal longitudinal separation is $\Delta\phi \approx 1.4^\circ$. The result of a simulation again using 10,000 observations (by each of the two satellites) to simulate the recovery of 10,000 East-West differences of the magnetic vector for such a separation is shown in Fig. 6b. This figure confirms that coefficients with high order are indeed better recovered with such a mission concept than with single-satellite mission concepts (recall Fig. 5a, in particular). Note however that Fig. 6b also shows that (as could have been expected from (7)) only relying on East-West differences of the magnetic vector does not make it possible to determine the zonal terms ($m = 0$). This issue can however be

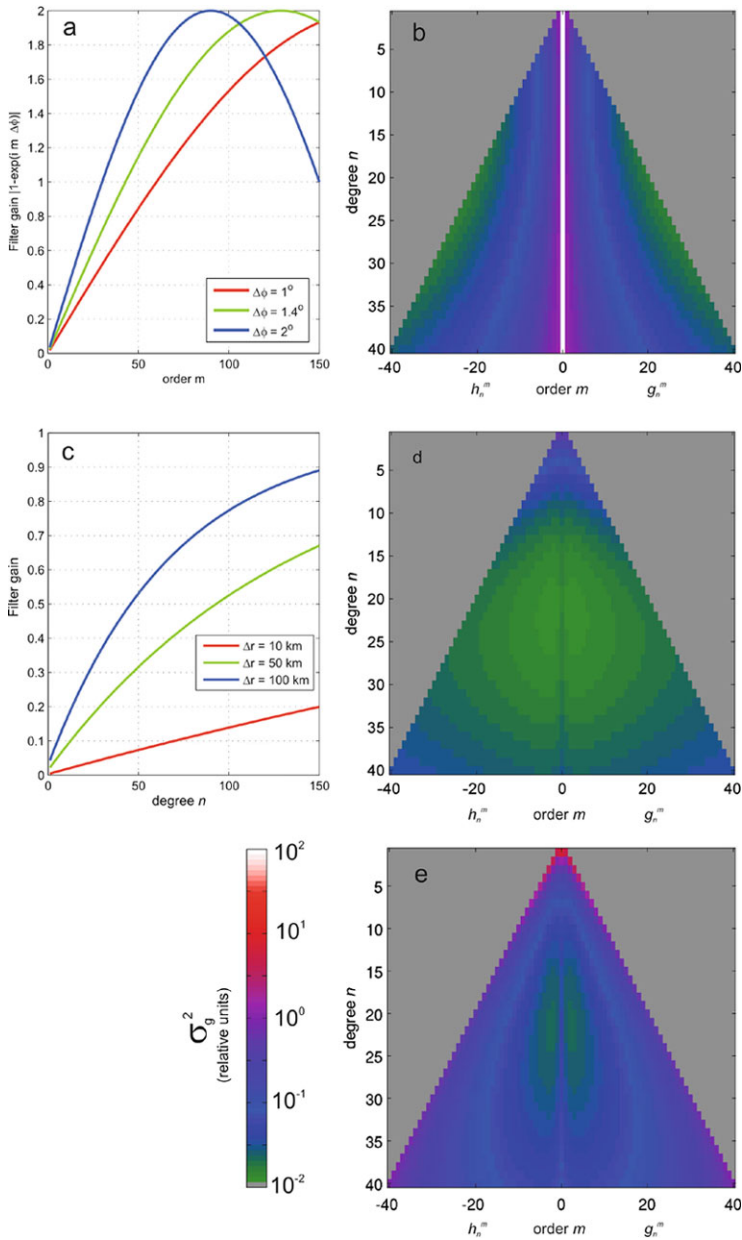


Fig. 6 (a): Relative sensitivity of the East-West magnetic difference versus spherical harmonic order m , for three different longitude separations, $\Delta\phi$. (b): Variance of the recovered Gauss coefficients when a $\Delta\phi = 1.4^\circ$ longitude separation is assumed between two close-by polar orbiting satellites (both at 450 km altitude) (c): Relative sensitivity of the radial magnetic difference versus spherical harmonic degree n , for three different radial separations, Δr . (d): Variance of the recovered Gauss coefficients when a $\Delta r = 50$ km altitude separation is assumed between two close-by polar orbiting satellites (the lower satellite being at 450 km altitude). (e): Variance of the recovered Gauss coefficients when a $\Delta\theta = 3.8^\circ$ latitude separation is assumed between two trailing polar orbiting satellites (at 450 km altitude)

circumvented by also making use of the individual vector measurements made by each of the two satellites, in addition to their East-West differences. Thus, smartly combining the advantages of a single satellite concept with the advantages of an East-West two-satellite gradient concept can lead to a much improved recovery of the field of internal origin. Such a possibility will be illustrated in more detail in Sect. 6, when discussing the upcoming *Swarm* satellite constellation.

Two other close-by LEO satellite concepts can also be envisioned. Similar to what was done in (7) for the East-West gradient of the magnetic field, it is for instance possible to investigate analytically the advantage of knowing the radial magnetic field gradient: The difference of the magnetic field at two satellites separated by Δr in altitude is $\Delta \mathbf{B} = \mathbf{B}(r, \theta, \phi) - \mathbf{B}(r + \Delta r, \theta, \phi) = -\text{Re}\{\nabla \Delta V\}$ which yields

$$\Delta \gamma_n^m = \left(1 - \left(\frac{r}{r + \Delta r} \right)^{n+2} \right) \gamma_n^m. \tag{8}$$

For small radial distances ($\Delta r \ll r$) the filter gain is $1 - \left(\frac{r}{r + \Delta r} \right)^{n+2} \approx (n + 2) \frac{\Delta r}{r}$ demonstrating that the radial gradient is sensitive to Gauss coefficients of higher *degree* n . The filter gain for various values of altitude separation as a function of spherical harmonic degree n is presented in Fig. 6c (the lower altitude satellite being at 450 km altitude), and the results of a simulation for a separation of 50 km is shown in Fig. 6d. This figure confirms that such a mission concept could also indeed improve on single-satellite mission concepts (recall Fig. 5a, in particular). However, it is important to note that such a concept would require a very significant difference in altitude between the two satellites, raising practical orbital issues. Two such freely orbiting satellites would indeed not orbit at the same speed, leading to significant drift in latitude between the two satellites, ruining the whole mission concept, unless fuel-costly orbital corrections are regularly implemented throughout the course of such a mission. Other options could be to rely on a (often considered perilous) tethered concept (as already proposed by e.g., Merayo et al. 1998 but never implemented), or a “cartwheel” configuration (e.g., Wiese et al. 2009), which would however not permanently maintain a pure radial gradient between the two satellites.

This finally leads us to consider yet a third concept based on two trailing LEO satellites orbiting along the same polar orbit and providing the possibility of measuring the North-South gradient of the magnetic field. No simple exact formula (such as equations (7) and (8) for the two previous cases) can then be derived (as taking derivatives along θ involves mixing spherical harmonics). But it can be anticipated that, as $P_n^m(\cos \theta)$ is proportional to $\sin(n\theta)$ (at least for high degrees n , orders $m \ll n$ and at non-polar latitudes), such a possibility would improve the recovery of high-degree Gauss coefficients. We also simulated such a situation, by assuming two trailing satellites on a polar orbit at 450 km altitude, separated by $\Delta \theta = 3.8^\circ$ in latitude (Fig. 6e). This corresponds to a one minute separation in time, and 460 km in space. As expected, such a concept would indeed enhance the recovery of Gauss coefficients with high n values, compared to single-satellite mission concepts (recall Fig. 5). But for lower degrees (for which the above stated approximation $P_n^m \propto \sin(n\theta)$ is not fulfilled) there is also a degradation of the near-tesseral terms. Of course, as in the case of the East-West gradient concept, this drawback could be compensated by also taking advantage of the individual vector measurements made by each of the two satellites. It is worth however noting that in the present case, both satellites would essentially provide the same geographical coverage (the trailing satellite following the same orbit as the leading satellite), which is a disadvantage. This disadvantage is one that led to favor the choice of an East-West gradient for the two lower satellites of the *Swarm* satellite constellation (Sect. 6).

As a matter of fact, relying on an East-West gradient concept also has the important advantage of better avoiding the highly dynamical, but mainly zonal, magnetospheric magnetic field, which is most systematically removed when computing East-West gradients of the field from synchronous data collected by both satellites.

5 Past and Present Successful Missions

5.1 *POGO* and *Magsat*

As already mentioned, the first successful LEO magnetometry satellites were the US *Polar Orbiting Geophysical Observatories (POGO)*, the low altitude half of the six Orbiting Geophysical Observatories (*OGO*) intended to investigate the Earth's magnetosphere and outer ionosphere (Jackson and Vette 1975). The corresponding three successive satellites measured the field from October 1965 to September 1967 (*OGO-2*), July 1967 to January 1969 (*OGO-4*) and June 1969 to June 1971 (*OGO-6*), with a few weeks of data overlap for *OGO-4* and *OGO-2*. All three satellites had similar orbits with perigee at about 400 km, apogee ranging from 910 km (*OGO-4*) to 1510 km (*OGO-2*), and inclinations between 82° (*OGO-6*) and 87.3° (*OGO-2*) (for more details see e.g. Cain 2007). They were equipped with optically pumped rubidium vapor absolute magnetometers and measured only magnetic field intensity. Intrinsic measurement error of all three satellites is believed to be below 1 nT, but contribution due to position uncertainty results in an effective magnetic error of about 4 nT (Sabaka et al. 2004). The interested reader can find the data at <ftp.space.dtu.dk/data/magnetic-satellites/POGO> (see also Cain and Sweeney 1973).

Despite their fairly elliptical orbits and the limitations linked to the intensity-only single-satellite concept (recall Sect. 3), these *POGO* satellites led to a number of scientific firsts. Combined with observatory data, their observations proved key to the establishment of the first International Geomagnetic Reference Field (Cain et al. 1967) and offered crucial constraints for reconstructing the core field evolution over the 1965–1971 time period (Sabaka et al. 2004). They also led to the first global magnetic anomaly map (Regan et al. 1975) and allowed some first observations of the field of external origin from space, such as that of the equatorial electrojet (Cain and Sweeney 1973). *POGO* data have also been used in many subsequent studies, in combinations with the data collected by more recent missions (see below), especially in the context of the investigation of the lithospheric field, the static (in fact, nearly static, see e.g. Hulot et al. 2009; Thebaud et al. 2009) nature of which makes it possible to take advantage of data collected at very different epochs (see e.g. Langel and Hinze 1998).

The next successful LEO magnetometry satellite was launched a little less than a decade later, again by the US. This satellite, *Magsat*, was the first to make precise, globally distributed measurements of the vector magnetic field at low altitude. It flew between October 1979 and June 1980, at an altitude between 350 and 550 km in a near-polar dawn-dusk orbit with an inclination of 97°. It was equipped with a scalar (cesium) magnetometer, and a tri-axial fluxgate magnetometer which sampled the field at 16 Hz with a resolution of ± 0.5 nT. Attitude was measured using two star-trackers on the spacecraft; transformation of attitude determined by these star trackers to the vector magnetometer located at the tip of the boom was done using a sophisticated optical system. Attitude errors limited the vector data accuracy to about 4 nT rms. See e.g. Langel et al. (1982c) and Purucker (2007) for more technical details, and <ftp.space.dtu.dk/data/magnetic-satellites/Magsat>, to access the data.

Because *Magsat* was the first LEO magnetometry mission based on a full-vector single-satellite concept, it was the first to provide enough information to overcome the *Backus*

effect that plagued the previous *POGO* program (recall Sect. 3). This technical progress quickly led to major achievements. In particular, *Magsat* made it possible to compute the first high degree and order models of the field of internal origin, highlighting the now well-known fact that at the Earth's surface, this field is dominated by the core field up to degree and order 13, and by the lithospheric field beyond degree and order 15 (Langel and Estes 1982). It also led to considerable improvement in the recovery and interpretation of detailed lithospheric magnetic anomaly maps (e.g. Langel et al. 1982a, 1982b; Achache et al. 1987; Cohen and Achache 1990; Arkani-Hamed et al. 1994; Ravat et al. 1995; see also Langel and Hinze 1998 for an extensive review of the many studies already published at the time). But *Magsat* also contributed significantly to studies of ionospheric and magnetospheric currents: from a determination of the meridional (toroidal) current system connected to the Equatorial Electrojet (Maeda et al. 1982), to the determination of the absolute strength of the magnetospheric ring-current during quiet conditions (Langel and Estes 1985), and an in-situ determination of *F*-region currents (Olsen 1997). Those progress finally also led to the initiation of CM types of approach for jointly modeling the field of internal and external origin, by making use of both LEO satellite and observatory data (Sabaka and Baldwin 1993; Langel et al. 1996).

5.2 Ongoing Satellite Missions: *Ørsted*, *CHAMP* and *SAC-C*

After the very successful *Magsat* mission, and despite several attempts to launch other similar follow-on missions, two decades elapsed before the launch of the next LEO magnetometry missions based on a full-vector single-satellite concept. This eventually happened in 1999 and 2000, with the successive launches of three such satellites: *Ørsted*, *CHAMP* and *SAC-C*, which started the *International Decade of Geopotential Field Research*. As of mid-2010, both *Ørsted* and *CHAMP* are still in operation and providing high-quality data.

The Danish *Ørsted* satellite was launched on February 23, 1999 into a near polar orbit with an inclination of 96.5°, a period of 100 minutes, a perigee at 650 km and an apogee at 860 km. The orbit plane is slowly drifting, the local time of the equator crossing decreasing by 0.91 min/day, having started from an initial local time of 02:26 for the south-going track. *Ørsted* is gravity gradient stabilized and attitude maneuvers are performed using magnetic torquers. It has a 8 m long boom, deployed shortly after the launch and carrying the magnetic field instruments. These consist in a proton precession Overhauser magnetometer (built by CEA/LETI, France, and provided by CNES) mounted at the tip of the boom and measuring the magnetic field intensity with a sampling rate of 1 Hz and an accuracy better than 0.5 nT. At a distance of 6 m from the satellite body is the optical bench with a CSC (Compact Spherical Coil) fluxgate vector magnetometer mounted closely together with a Star Imager. The CSC samples the magnetic field at 100 Hz (burst mode, at polar latitudes) or 25 Hz (normal mode) with a resolution better than 0.1 nT. The instrument is calibrated against the field intensity measured by the scalar magnetometer. After calibration, the agreement between the two magnetometers is better than 0.33 nT rms. Due to attitude errors, the accuracy of the vector components (B_r , B_θ , B_ϕ) is limited to 2 to 8 nT (4 nT rms), depending on component. Nominal lifetime of the mission was 14 months, but after more than 11 years in space the satellite is still healthy and providing high-precision magnetic data. Since 2004 however, only intensity data are available. See Neubert et al. (2001), Olsen (2007) for more information and ftp.space.dtu.dk/data/magnetic-satellites/Oersted to access the data.

A copy of the *Ørsted* boom and payload (but with a US Scalar Helium Magnetometer instead of the CEA/LETI Overhauser magnetometer) was launched in November 2000 onboard the Argentinean satellite *SAC-C*. This satellite is in a circular sun-synchronous orbit

at an altitude of about 700 km and local time of 10:30/22:30. Unfortunately, due to a broken connection in a coaxial cable, no high-precision attitude data (and hence no reliable vector data) have been recovered. Intensity data nevertheless exist for the period January 2001 to December 2004 and are available at <ftp.space.dtu.dk/data/magnetic-satellites/SAC-C>.

The much more successful German *CHAMP* satellite was launched on July 15, 2000 on an almost circular, near polar (inclination 87.3°) orbit with an initial altitude of 454 km, which had decreased to about 270 km by July 2010. *CHAMP* advances one hour in local time within eleven days. Instrumentation is very similar to that of *Ørsted*; however, attitude is now obtained by combining measurements taken by two star imager heads, to minimize attitude error anisotropy. This leads to vector components recovered to better than 2 nT when attitude is measured by both star imager heads (which happens for more than 60% of the time). Otherwise the same accuracy is achieved as for *Ørsted*. Accuracy of the scalar measurements is also similar to that of *Ørsted* (better than 0.5 nT). Just like *Ørsted*, *CHAMP* is still healthy and providing both vector and intensity data. However, it is expected to re-entry Earth's atmosphere in the fall of 2010. See Reigber et al. (2002), Maus (2007a) for more information and <http://isdc.gfz-potsdam.de/champ/> to access the data.

It is important to stress that although based on the same basic full-vector single-satellite concept as *Magsat*, both *Ørsted* and *CHAMP* missions have crucial new characteristics that improve considerably on the original *Magsat* concept. Beyond the fact that both those satellites have been designed to make better quality measurements, their orbits have indeed been carefully chosen so as to avoid what ended up being one of the main limitations of the *Magsat* concept: the sun-synchronous characteristic of its dawn-dusk orbit. The drawback of such an orbit cannot be inferred from the simplified discussion of Sect. 3, as it is related to the spatio-temporal characteristics of the field of external origin, which we ignored altogether. This field has a significant sun-synchronous component of ionospheric origin, with non-zero dawn and dusk components which *Magsat* always saw as a systematic signal added to the field of internal origin. Although this systematic ionospheric signal is not exactly the same at dawn and dusk, averaging measurements taken over the same region at dawn and dusk cannot be used to entirely remove this signal (see e.g. Langel and Hinze 1998). In addition, associated externally induced internal sun-synchronous fields are also produced (see e.g. Tarits and Grammatica 2000; Grammatica and Tarits 2002), which *Magsat* could not possibly distinguish from the signal produced by the lithospheric field. This issue is no longer as severe for *Ørsted* and particularly *CHAMP* which explore all local times and also give access to night times (with much weaker ionospheric signal).

Another important innovative aspect of *Ørsted* and *CHAMP* is that they were both designed to operate over a much more significant period of time. In the case of *Ørsted*, this is mainly because *Ørsted* was launched at a higher altitude than *Magsat*. But this high altitude orbit has the disadvantage of making *Ørsted* less sensitive to the shortest wavelengths of the field of internal origin than *Magsat*. The very different design of *CHAMP* made it possible to combine the advantages of a long-lasting mission with that of a low altitude orbit. This was achieved by giving the satellite a much higher weight (522 kg), a small cross-section and some fuel to maintain the altitude, despite the considerable drag of the atmosphere at such a low altitude (which was the cause for the short duration of the *Magsat* mission). In addition, atmospheric re-entry of *Magsat* was during a period of high solar activity (and thus increased air-drag) compared to *CHAMP* for which the very last low-altitude data are measured during low solar activity.

As *Ørsted* was the first full-vector mission to be launched nearly twenty years after *Magsat*, it was also the first to witness the very significant changes that had occurred in

the core field during that period of time, particularly in the medium spatial scales that could not be monitored from ground observatories (Hulot et al. 2002), initiating renewed interest in the investigation of the core surface flows (e.g. Eymin and Hulot 2005), and other possible mechanisms (Jackson 2003) responsible for such changes. It also led to the first demonstration that high degree secular variation models could be constructed from such long-lasting single satellite missions (Olsen 2002). Although *Ørsted*'s high altitude orbit was not optimized for the recovery of the lithospheric field, it also made it possible to quickly confirm the early lithospheric field maps derived from *Magsat*, and improve on our understanding of the respective roles of induced and remanent magnetization in the production of this field (Purucker et al. 2002). Finally, it also made it possible to further progress on the nature of field of external origin, particularly the field-aligned currents (e.g. Papitashvili et al. 2001; Christiansen et al. 2002; Neubert and Christiansen 2003).

When *CHAMP* was launched a year and a half after *Ørsted*, it also led to additional major breakthroughs. As expected, its much lower orbital altitude quickly made it possible to produce a much improved lithospheric field model (Maus et al. 2002). But *CHAMP* also led to new observations of ionospheric effects in the *F*-region (Lühr and Maus 2006), in particular the observation of significant magnetic signature of night-time currents (Maus and Lühr 2006), of a so-called "diamagnetic effect" (Lühr et al. 2003), and of the magnetic signature of equatorial plasma instabilities (Stolle et al. 2006). Finally *CHAMP* also led to the first unambiguous and elegant demonstration that the magnetic field produced by the oceans (in the present instance, by tide motions) contribute to (and can be detected in) the field measured from space (Tyler et al. 2003).

In the years that followed and until now, much advantage was subsequently taken of the accumulation of data from both *Ørsted* and *CHAMP*, and to a lesser extend, *SAC-C*, in the context of what is now known as the *International Decade of Geopotential Field Research* (Friis-Christensen et al. 2009). This led in particular to a continuous stream of ever improving models of the lithospheric field (for a recent review, see e.g. Thébaud et al. 2010), and of the core field, the time variations of which are now monitored with unprecedented accuracy (see e.g. Gillet et al. 2010). This also led to more and more detailed investigations of the core dynamics responsible for these variations (see e.g. Finlay et al. 2010), and definitely demonstrated the unique advantage of LEO satellites for continuously monitoring the Earth's magnetic field, particularly in view of possibly forecasting its future evolution with the help of data assimilation techniques (see e.g. Fournier et al. 2010).

Before turning to the soon to be launched ESA *Swarm* constellation mission, it is worth pointing out that the simultaneous availability of *Ørsted*, *CHAMP* and *SAC-C* data (the result of a very long delay in the launch of *Ørsted*) already provided an example of what can be achieved with a small constellation of satellites. The fact that *Ørsted* and *CHAMP* orbited in very different orbital planes indeed proved very useful, already leading to substantial progress in the modeling of the various fields along the CM approach (see e.g. Sabaka et al. 2004). But it is equally important to stress that this constellation was not yet optimal, as it could not be used for gradient measurement purposes.

Attempts to test gradient concepts analogous to those discussed in Sect. 4 have nevertheless recently been made with the help of the experimental US *Space Technology 5 (ST-5)* constellation. This constellation consisted in three very light (less than 25 kg) spinning micro-satellites, who collected vector magnetic field observations with miniature tri-axial fluxgate magnetometers. This mission was launched on 22 March 2006 and operated for 90 days. It was mainly technology oriented, and meant to test the possibility of operating such small satellites as a constellation and recover potentially useful magnetic data (see Slavin et al. 2008). As the satellites were spinning quite fast (0.33 Hz), did neither carry any

GPS receiver nor a star imager for attitude determination, and were trailing each other on a very elliptical orbit (300–4500 km, 105.6° inclination), they were much better suited for the investigation of field-aligned currents than for the recovery of the field of internal origin. Nevertheless, a subset of the data collected at altitude below 800 km by the two closest satellites (with a separation distance comparable to their altitude) could be used to produce some North-South gradient estimates of the field intensity over mid and high-northern latitudes (Purucker et al. 2007). The main conclusion of this study is that those gradient estimates succeeded at providing data of quality superior to that of *Magsat*, even though the individual data provided by each satellite were of poorer quality, thus confirming the potential advantage of using gradient data.

6 The Near Future: *Swarm*

Except in the case of the *ST-5* constellation mission just discussed, all past and present LEO magnetic satellites were initially designed as single spacecraft missions. A constellation consisting of several satellites opens, however, new possibilities for exploring the geomagnetic field from space.

At first glance one would expect that using simultaneous data from N satellites results in a reduction of the error σ_g of the Gauss coefficients by \sqrt{N} , since the amount of data is increased by N compared to one single satellite. This error reduction by \sqrt{N} of course only holds if the data are statistically independent, which is highly idealistic and unrealistic since the main limiting factor for improved field modeling is not the measurement error but the dynamic behavior of external sources. Treating data from a constellation of N satellites in a “single-satellite” approach thus typically results in an improvement of the model error by less than \sqrt{N} .

However, if *explicit* advantage is taken of the constellation, there is some potential for model improvement better than \sqrt{N} . This point was already illustrated in Sect. 4 when we discussed two-satellite gradient concepts. But advantageous concepts based on even more satellites can also be designed. Unfortunately the cost of implementing such concepts increases with the number of satellites to be launched, and some compromises have to be found so that each considered additional satellite brings an optimal improvement. The latest such optimal concept is the three-satellite constellation *Swarm* concept soon to be launched by ESA, which we will now discuss. In what follows, we first briefly describe the *Swarm* constellation concept (Sect. 6.1) and then proceed to give a brief account of the various simulations that have been carried out to illustrate its usefulness (Sect. 6.2).

6.1 The Three-Satellite *Swarm* Concept

Swarm was selected by the European Space Agency (ESA) in 2004 and is now scheduled for launch in mid 2012. The mission comprises a constellation of three satellites, with two spacecraft to be launched side-by-side at low altitude to measure the East-West gradient of the magnetic field, and a third spacecraft to be launched (with the same launcher) at a slightly higher altitude. The orbital plane of this third spacecraft will progressively shift with respect to the orbital plane of the lower spacecraft pair, to provide data at different local times. More details about the mission can be found in Friis-Christensen et al. (2006, 2009).

Figure 7 shows two of the three identical *Swarm* satellites with their main instruments. Their overall design is inspired from that of *CHAMP* to again ensure a long lifetime in orbit (a nominal lifetime of 4.5 years). The primary goal of *Swarm*, measuring the vector

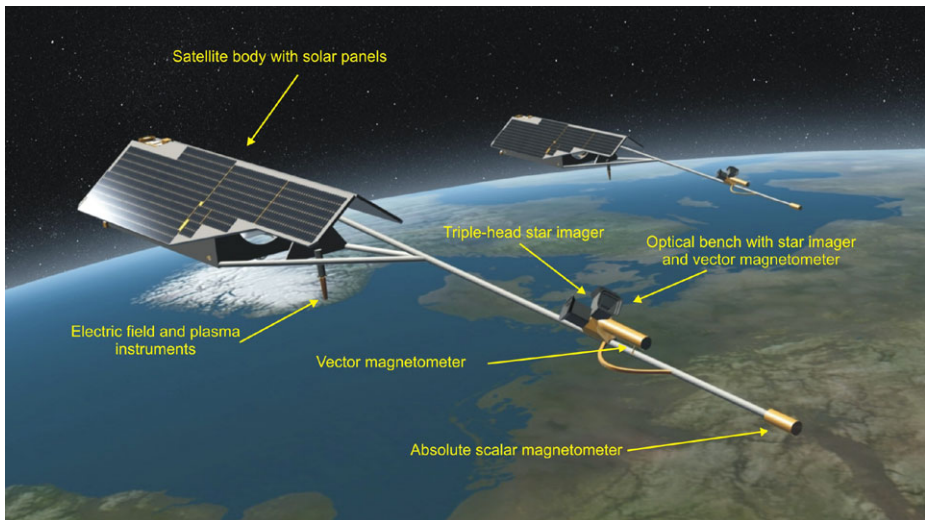


Fig. 7 Two (out of three) *Swarm* satellites

components of the magnetic field with high-precision, requires the combination of three instruments: an absolute scalar magnetometer, a vector magnetometer, and a star imager to provide the attitude of the vector magnetometer. As we saw, high-quality instruments for that purpose have already been developed for the purpose of the *Ørsted* and *CHAMP* missions. However, *Swarm* is the most ambitious project so far regarding accurate measurements of the Earth's magnetic field, and the desired magnetic field accuracy is significantly higher than that of those previous missions.

The vector magnetometers and star imagers are built by DTU Space (Copenhagen/Denmark), while the absolute magnetometer, a latest generation Helium 4 optical pumping absolute magnetometer built by LETI/CEA (Grenoble/France), is provided by CNES, the French space agency. Precise orbit information will be provided by GNSS receivers. As *Swarm* also aims at investigating electrical currents in the ionosphere and their effect on the Earth environment, the payload will also include a tri-axial accelerometer, built by the Czech Aeronautical Research and Test Institute VZLU (Prague/Czech Republic), an instrument to measure the electric field, built by the University of Calgary (Canada), and a Langmuir probe from the Swedish Space Institute (Uppsala/Sweden) for measuring plasma density.

Design of the constellation formation is an important issue, and the selected constellation reflects an attempt to maximize the scientific benefit for the various research objectives. The benefit of various constellation scenarios has been studied in full mission simulations (an example of such a simulation is given in Sect. 6.2 below) and the following constellation has finally been selected for implementation (see Fig. 8):

- One pair of side-by-side satellites (*Swarm* A+B) to be launched in near-polar, circular orbits with initial altitude and inclination of 450 km and 87.4°, respectively; the East-West separation between the satellites will be about 1.4° in longitude (corresponding to 160 km near the Equator), and the expected atmospheric re-entry at the end of the 4.5 year mission lifetime will make it possible to measure the magnetic field from rather low altitudes (below 300 km), which is beneficial for an improved lithospheric field determination.

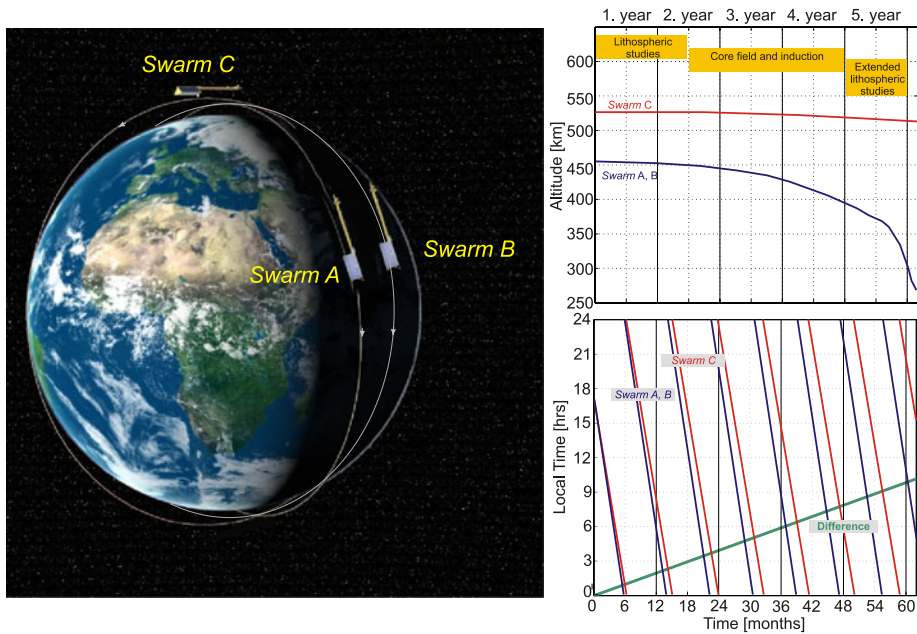


Fig. 8 Impression of the proposed three satellite constellation (*left*) and mission scenario (*right*). Local time evolution for the satellites in the two orbital planes (*right bottom*); change in altitude versus time (*right top*)

- A third, higher, satellite (*Swarm C*) to be launched simultaneously in a circular orbit with 88° inclination at an initial altitude of 530 km; the right ascension of the ascending node will be drifting somewhat more slowly than that of the two lower satellites, thus building up a difference of 6 hours in local time after 3 years (right panel of Fig. 8).

The two lower (*Swarm A+B*) satellites will thus be in an East-West gradient configuration, the advantage of which for recovering the small scales of the lithospheric field has already been discussed in Sect. 4. The additional higher satellite (*Swarm C*) will allow, in combination with data from the lower pair, for an enhanced description of the space-time structure of large-scale external currents, which is crucial for accurate separation of internal and external fields. The combination of close-by flying satellites (*Swarm A and B*) and different local time orbits (*Swarm A/B* compared to *Swarm C*) is thus beneficial for different research objectives.

6.2 Swarm End-to-End Mission Simulation

Contrary to the simple mission simulation discussed in Sects. 3 and 4 where external field contributions had been ignored for simplicity, this section reports on the until now most complete mission simulation performed for a LEO magnetic satellite mission. As part of the preparation of the *Swarm* mission, a full simulation was indeed carried out in order to assess the expected performance of the mission for the recovery of its primary science goals, namely, the core field and its secular variation during the mission lifetime, together with the small-scale lithospheric field. The study consisted in a set of analyses performed on measurements synthesized from the constellation ephemerides over the nominal 4.5 years lifetime of the mission. Synthetic magnetic signals were generated for all relevant contributions

to Earth's magnetic field: core and lithospheric fields, fields due to currents in the ionosphere and magnetosphere, to their secondary, induced, currents in the oceans, lithosphere and mantle, and fields due to currents coupling the ionosphere and magnetosphere. Details about the way these signals have been generated can be found in Sabaka and Olsen (2006) and Olsen et al. (2004, 2007), where many more detailed results of the simulations reported here can also be found. Note that as these simulations required the use of as realistic as possible conditions of the Earth's environment to be encountered by *Swarm*, geomagnetic and solar activity indices covering the time period from 1998.5 to 2003.0 have been used, to mimic those solar-driven conditions, had *Swarm* been launched in mid-2009 (one solar cycle later than 1998.5) as originally planned. Realistic instrument noise was also included from what is known from the *CHAMP* satellite; a mission whose equipment is very similar to that of *Swarm*.

The Comprehensive Model (CM) inversion approach (Sabaka et al. 2002, 2004) was applied to this synthetic data in order to recover the underlying input models, and an assessment of the recovery was done by comparing original and retrieved models. As already mentioned in Sect. 2, the philosophy of the CM approach is to parameterize and co-estimate all major field sources from the measurements, thus providing optimal signal separation by accounting for possible spatio-temporal cross-correlations. This is particularly important since, as noted in Sect. 1, these field sources overlap on both spatial and temporal scales. In particular, the CM approach takes advantage of the fact that a sufficiently dense sampling of vector data at satellite altitude will, in theory, allow separation of the external magnetospheric field from the remaining internal field sources. It also can take advantage of data from ground-based networks, such as magnetic observatories, which aid to separating the ionospheric field from the core, lithosphere, and induced fields, though these do not allow a complete separation at all spatial scales of interest. However, one can further invoke the temporal properties of the fields, such as the dominant sun-synchronous modes of the ionosphere and its near absence in the nightside sector (at least at low-mid latitudes) versus the slowly-varying or nearly constant nature of the core and lithospheric fields. If one has information on conductivity structure, particularly in the upper-mantle, then this may be used to further couple the induced and inducing fields, and consequently help separate them from other internal fields.

Although parameter cross-correlation and data selection are important to consider in isolating target signals, one has further options if contemporaneous multi-point observations are available from a satellite constellation such as *Swarm*. As we saw in Sect. 4, relying on gradient measurements, or more generally, linear combinations of measurements has the potential to greatly boost the signal-to-noise ratio and thus enhance the recovery of certain target signals at certain spatial wavelengths and of the corresponding Gauss coefficients. The problem, however, is that complementary Gauss coefficients will often suffer by a corresponding decrease in signal-to-noise ratio (as was for instance the case for the low order m Gauss coefficients in the simplified East-West gradient mission simulation we reported in Sect. 4, recall Fig. 6b). The *Swarm* End-to-End simulator study (Olsen et al. 2007) addressed this problem with a technique called *Selective Infinite Variance Weighting* (SIVW). The focus of that study was to recover the small-scale lithospheric field signals from differences of vector measurements from the *Swarm* satellite low pair while recovering all other fields from the complementary data (sums of the data provided by the low pair of satellites, complemented by the data provided by the high satellite) in an optimal way. This was achieved by introducing a set of nuisance lithospheric parameters (biases) for spherical harmonic orders above 20, which only directly affect the complementary data. This is equivalent to assigning infinite variance to a noise process that contaminates the lithospheric at this scale in this data (see Olsen et al. 2007 for technical details).

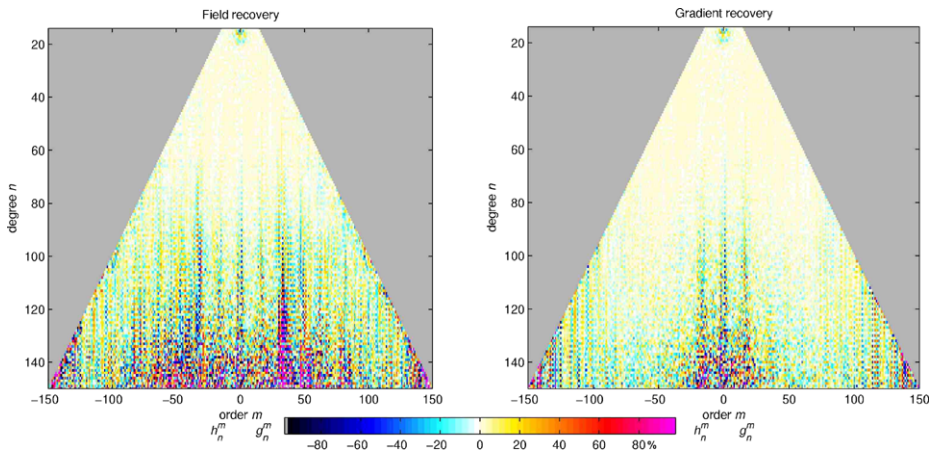


Fig. 9 Sensitivity matrix: Relative error (normalized difference between original input and recovered value) of each coefficient in dependence on spherical harmonic degree n and order m for the retrieval of the lithospheric field from simulated *Swarm* data by means of CM. *Left*, when no gradient information is exploited; *right*, when gradient information with SIVW is used (see text for details)

As an example of the benefits of the SIVW technique described above, Fig. 9 shows triangular plots of degree-normalized error for the lithosphere when no gradient information is exploited (left) and when gradient information with SIVW is used (right). (Note that here we show triangular plots of the error (difference between input and recovered model), in contrast to the triangular plots of Figs. 5 and 6 which shows the variances of the recovered Gauss coefficients.) Taking explicit advantage of the gradient measurements (right panel) results in a significant improvement in recovery for orders above 20 and no degradation below. This general behavior of no degradation is also seen (but not shown) in the recovery of other fields, such as the magnetosphere and high-frequency internal signals.

To illustrate in a somewhat less technical way the benefit *Swarm* is expected to bring in terms of improving the recovery of the lithospheric field, Fig. 10 shows the increased spatial resolution of the lithospheric field as more accurate magnetic measurements became available since the early times of *POGO* and *Magsat*. Only lithospheric field structures larger than 1000 km (corresponding to spherical harmonic degrees $n \leq 40$) could be resolved with these satellites, as illustrated in the upper panel of the figure, which shows the radial component B_r of the field of internal origin (after removal of degrees $n = 1$ to 15, dominated by the core field) at Earth's surface, as given by the spherical harmonic model derived by Cain et al. (1985). In addition to the limited resolution, errors in the estimated spherical harmonic terms prevented any clear difference between the lithospheric field strength over continental and oceanic regions to be detected. Such a difference, however, has since clearly been found from an analysis of *Ørsted* and *CHAMP* data. These missions made it possible to improve the resolution to about 500 km (corresponding to $n \leq 80$), as illustrated by the middle panel of the figure, which now shows B_r as given by the MF6 model of Maus et al. (2008). With *Swarm*, it is expected that structures down to at least 300 km scale size (corresponding to $n = 133$, as suggested by Fig. 9) will be resolved. The impact such a progress would bring is illustrated in the bottom panel of Fig. 10, which is based on the combination of a synthetic field model for $n > 80$ and of MF6 for $n \leq 80$ (the combined model that was used for the purpose of the simulation illustrated in Fig. 9, see Olsen et al. 2007). Such a considerably improved map would then make it possible to reduce the gap between the

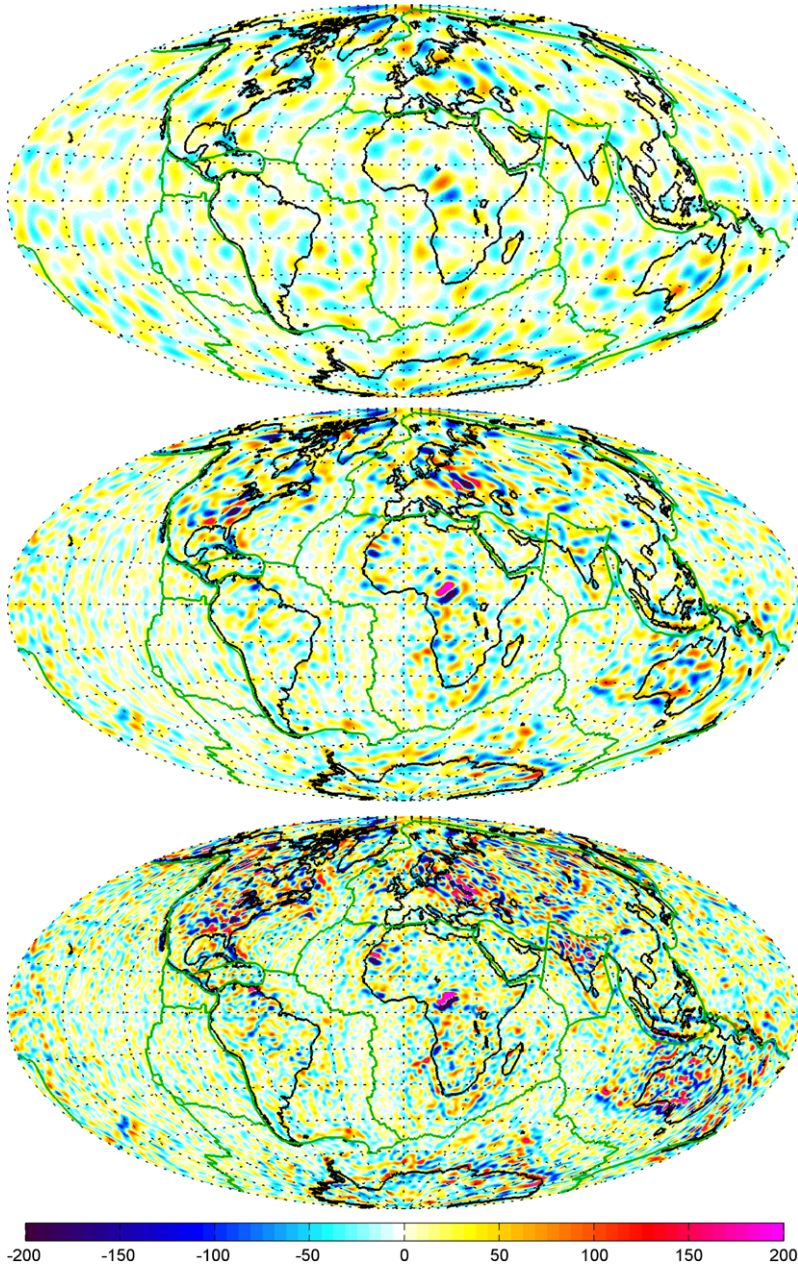


Fig. 10 Radial component of the lithospheric field (in nT) at Earth surface (spherical harmonics $n = 16 - N_{\max}$) showing the improvement of lithospheric field determination. *Top panel:* based on POGO and Magsat data ($N_{\max} = 40$, after Cain et al. 1985). *Middle panel:* current status, based on CHAMP observations ($N_{\max} = 80$, after Maus et al. 2008). *Bottom panel:* resolution to be expected from data of the upcoming Swarm constellation mission ($N_{\max} = 133$)

smallest spatial scales of the lithospheric field that can be recovered from sea and air regional magnetic surveys, and the largest scales already resolved by *CHAMP* (see e.g. Maus et al. 2009). Reducing this gap, and eventually removing it altogether, is a major goal, as it would then make it possible to build the first entirely data-derived World Digital Magnetic Anomaly Map (WDMAP, see e.g., Korhonen et al. 2007), a map of major interest for the understanding of the structure and dynamics of the lithosphere.

But *Swarm* will not only allow for enhanced determination of internal sources. It will also make it possible to further improve our understanding of the external sources. As shown by Ritter and Lühr (2006), combining the East-West gradient measured by the lower satellite pair with an estimation of the North-South gradient obtained by taking time differences of the vector measurements, will for instance make it possible for instantaneous *in-situ* radial current densities at high-latitudes to be estimated. The method has also been tested using synthetic *Swarm* satellite magnetic vector data, and a generally good agreement between input and recovered radial current density on an orbit-by-orbit basis could be achieved.

In a somewhat complementary fashion, and as has also been tested with *Swarm* synthetic data (Tøffner-Clausen et al. 2010), the combination of data obtained at different local times—recall from the bottom right part of Fig. 8 that the local time difference between the upper and lower satellites 3 years after launch will be about 6 hrs corresponding to 90° in longitude—will also allow for an improved determination of the spatial structure of large-scale external, and especially of magnetospheric, fields. In fact, the accurate recovery of time-series of not only magnetospheric but also high-frequency internal signals is also crucial for probing the mantle conductivity structure, and this too has been shown to be feasible with *Swarm* synthetic data (Kuvshinov et al. 2006), again illustrating the benefit of the three-satellite constellation concept selected for *Swarm*.

7 Outlook

What after *Swarm*? Given the importance of permanently monitoring the Earth's magnetic field from space, as very clearly demonstrated by the considerable success of the *International Decade of Geopotential Field Research* so far, it is indeed of primary importance to already start thinking about ways to further improve on the *Swarm* concept, for a much needed successor by the time the mission ends (after 2016).

An obvious way to possibly go is to consider a concept involving at least one more satellite. One drawback of the side-by-side East-West gradient configuration chosen for the low-pair satellites of *Swarm*, is that it is less sensitive to East-West than to North-South oriented lithospheric field structures. Enhancing this sensitivity would clearly require measurements of the North-South (or, alternatively, of the radial) magnetic field gradient. Indeed, as was discussed in Sect. 4 (though in terms of the sensitivity with respect to the Gauss coefficients to be recovered), adding the possibility of such gradient measurements, would clearly provide ways of increasing the return of an improved mission.

It is interesting to note that similar considerations have driven the evolution of gravity space missions. Looking at the analogy between missions for exploring Earth's magnetic and gravity fields is instructive in this context. While *Ørsted* and *CHAMP* (which also measures the gravity field thanks to an onboard accelerometer), are examples of satellites measuring the vector field only, *GRACE* (Tapley et al. 2004) and *Swarm* were both designed to also measure one component of the field gradient (in the case of *GRACE*, a quantity related to the North-South gradient of the gravity field). However the latest mission concept

of *GOCE* (Drinkwater et al. 2003) already measures the full gravity gradient tensor (tensor of all second space derivatives of the gravity potential). Aiming at measuring the analogous magnetic gradient tensor (nine component tensor of all three spatial derivatives of all three components of the magnetic field) would thus be a natural next step. In addition to an enhanced high-resolution mapping of the lithospheric magnetic field, such gradient measurements would in fact also allow for an improved in-situ determination of the electric current density in the near-Earth environment. Indeed, such in-situ determinations of currents in the far-Earth environment (at distances of several Earth radii) have already been obtained with magnetic data taken by ESA's four satellite *Cluster* constellation mission (Balogh et al. 1997), and several dedicated techniques (e.g. the "curlometer", cf. Dunlop et al. 2002) have been developed for that purpose. Similar techniques could thus also be applied to magnetic gradient tensor measurements taken in the near-Earth environment.

Measuring the full magnetic gradient tensor by one single spacecraft (as done by *GOCE* for the gravity gradient tensor) is a major technical challenge which may in fact not even be appropriate, given the specificity of the multiple magnetic sources. But a more appropriate approach could consist in relying on constellations of multiple satellites at distances of tens to hundreds of kilometers. A particularly attractive possibility would be one relying on satellites flying in a "cartwheel" configuration, with each of the individual satellites orbiting on a well designed slightly elliptical orbit such that their global center of mass evolves along a circular orbit (Wiese et al. 2009). In such a configuration, two satellites which would jointly provide a measure of the radial gradient of the field at some initial point on the orbit of the center of mass (and at its antipode), would then next be able to jointly provide a measure of the along-track (North-South) gradient of the field at a point located 90° away from this initial point (and at its antipode). Even better, flying three satellites (in the same orbital plane) in an optimized cartwheel configuration could allow for simultaneous measurements of field gradients along three different directions in the orbital plane. Adding a fourth satellite in a slightly different orbital plane could then finally also allow for a determination of the East-West gradient of the field. Such a four-satellite constellation would therefore be able to provide nine different measures of the magnetic gradient tensor in the 3D space, thus allowing for the reconstruction of the full tensor. (Note that in addition, advantage could further be taken of the fact that even in the general case with in-situ electrical currents, there are only 8 independent elements of the magnetic gradient tensor, because of $\text{div}\mathbf{B} = 0$, cf. Olsen and Kotsiaros (2010).)

Constellation flying is, however, very demanding in terms of satellite control. In this respect, a "fleet" of free-flying satellites measuring the field at various altitudes and local times (as opposed to a constellation with control of inter-satellite distances) could also be considered. By combining the measurements taken by various satellites it would still be possible to obtain gradient information at some points in space and time. But the specific advantage of such a many free-flying satellite configuration would mainly lie in its ability to better determine the large-scale magnetospheric currents, which still currently constitute a major source of errors for modeling the geomagnetic field. In fact, if any even more ambitious concept could possibly be implemented, there is no doubt that adding at least one constellation of four satellites (in the configuration described in the previous paragraph) to such a fleet, would provide a most optimal scientific return.

Finally, it is worth recalling that measuring the magnetic field intensity can still be highly beneficial from a scientific point of view, and technically much simpler and cheaper, if low latitudes vector data are also available to alleviate the *Backus effect* (recall Sect. 3). A combination of a few very cheap polar orbiting scalar-only satellites augmented by a low-inclination satellite measuring the field vector could be a good and relatively cheap

compromise. This would at least ensure a permanent monitoring of the geomagnetic field from space, with comparable and perhaps even enhanced quality to what has already been achieved with *Ørsted* and *CHAMP*.

Each of the above outlined mission scenarios would certainly deserve some further investigation to better assess their feasibility, cost and specific advantages in terms of scientific return. What can nevertheless be stated for sure from what has already been learned over the past 50 years of space LEO magnetometry is that independently of the concept finally retained for future implementation, continuation of magnetic field observation from space remains a very high scientific priority.

Acknowledgement The authors are very grateful to Andre Balogh, Roger-Maurice Bonnet and the International Space Science Institute for inviting them to take part in the Terrestrial Magnetism Workshop held in Bern in March 2009. They would like to also thank Mike Purucker and Vincent Lesur for stimulating discussions on various issues discussed in this chapter. GH acknowledges partial support from CNES. This is IGP contribution 3052.

References

- J.A. Achache, A. Abtout, J.L.L. Mouël, The downward continuation of MAGSAT crustal anomaly field over Southeast Asia. *J. Geophys. Res.* **92**, 11584–11596 (1987)
- P. Alberto, O. Oliveira, M.A. Pais, On the non-uniqueness of main geomagnetic field determined by surface intensity measurements: the Backus problem. *Geophys. J. Int.* **159**, 558–554 (2004). doi:[10.1111/j.1365-246X.2004.02413.x](https://doi.org/10.1111/j.1365-246X.2004.02413.x)
- J. Arkani-Hamed, R.A. Langel, M. Purucker, Scalar magnetic anomaly maps of Earth derived from POGO and Magsat data. *J. Geophys. Res.* **99**(B12), 24–075 (1994)
- G.E. Backus, Non-uniqueness of the external geomagnetic field determined by surface intensity measurements. *J. Geophys. Res.* **75**(31), 6339–6341 (1970)
- A. Balogh, M. Dunlop, S. Cowley, D. Southwood, J. Thomlinson, K. Glassmeier, G. Musmann, H. Lühr, S. Buchert, M. Acuna, D.H. Fairfield, J.A. Slavin, W. Riedler, K. Schwingenschuh, M.G. Kivelson, The Cluster magnetic field investigation. *Space Sci. Rev.* **79**(1), 65–91 (1997)
- J.C. Cain, POGO (OGO-2, -4 and -6 spacecraft), in *Encyclopedia of Geomagnetism and Paleomagnetism*, ed. by D. Gubbins, E. Herrero-Bervera (Springer, Heidelberg, 2007)
- J.C. Cain, R.E. Sweeney, The POGO data. *J. Atmos. Terr. Phys.* **35**, 1231–1247 (1973)
- J.C. Cain, S.J. Hendricks, R.A. Langel, W.V. Hudson, A proposed model for the International Geomagnetic Reference Field-1965. *J. Geomagn. Geoelectr.* **19**, 335–355 (1967)
- J.C. Cain, D.R. Schmitz, L. Muth, Small-scale features in the Earth's magnetic field observed by MAGSAT. *J. Geophys. Res.* **89**, 1070–1076 (1985)
- S. Chapman, J. Bartels, *Geomagnetism*, vol. I+II (Clarendon, Oxford, 1940)
- F. Christiansen, V.O. Papitashvili, T. Neubert, Seasonal variations of high-latitude field-aligned currents inferred from Ørsted and Magsat observations. *J. Geophys. Res.* **107**(A2), 1029 (2002). doi:[10.1029/2001JA900104](https://doi.org/10.1029/2001JA900104)
- Y. Cohen, J. Achache, New global vector magnetic anomaly maps derived from Magsat data. *J. Geophys. Res.* **95**, 10783–10800 (1990)
- S. Constable, Geomagnetic induction studies, in *Treatise on Geophysics*, vol. 5, ed. by M. Kono (Elsevier, Amsterdam, 2007), pp. 237–276
- S. Dolginov, L.N. Zhuzgov, N.V. Pushkov, L.O. Tyurmina, I.V. Fryazinov, Some results of measurements of the constant geomagnetic field above the USSR from the third artificial Earth satellite. *Geomagn. Aeron.* **2**, 877–889 (1962)
- M. Drinkwater, R. Floborghagen, R. Haagmans, D. Muzi, A. Popescu, GOCE: ESA's first earth explorer core mission. *Space Sci. Rev.* **108**(1), 419–432 (2003)
- M. Dunlop, A. Balogh, K. Glassmeier, P. Robert, Four-point Cluster application of magnetic field analysis tools: The Curlometer. *J. Geophys. Res.* **107**, 1384 (2002). doi:[10.1029/2001JA005088](https://doi.org/10.1029/2001JA005088)
- C. Eymin, G. Hulot, On core surface flows inferred from satellite magnetic data. *Phys. Earth Planet. Inter.* **152**(3), 200–220 (2005). doi:[10.1016/j.pepi.2005.06.009](https://doi.org/10.1016/j.pepi.2005.06.009)
- C.F. Finlay, M. Dumberry, A. Chulliat, A. Pais, Short timescale core dynamics: theory and observations. *Space Sci. Rev.* (2010, in review)

- A. Fournier, G. Hulot, D. Jault, W. Kuang, A. Tangborn, N. Gillet, E. Canet, J. Aubert, F. Lhuillier, An introduction to data assimilation and predictability in geomagnetism. *Space Sci. Rev.* (2010). doi:[10.1007/s11214-010-9669-4](https://doi.org/10.1007/s11214-010-9669-4)
- E. Friis-Christensen, H. Lühr, G. Hulot, *Swarm*: A constellation to study the Earth's magnetic field. *Earth Planets Space* **58**, 351–358 (2006)
- E. Friis-Christensen, H. Lühr, G. Hulot, R. Haagmans, M. Purucker, Geomagnetic research from space. *EOS Trans. AGU* **90**(25), 213–215 (2009)
- N. Gillet, V. Lesur, N. Olsen, Geomagnetic core field secular variation models. *Space Sci. Rev.* (2010). doi:[10.1007/s11214-009-9586-6](https://doi.org/10.1007/s11214-009-9586-6)
- N. Grammatica, P. Tarits, Contribution at satellite altitude of electromagnetically induced anomalies arising from a three-dimensional heterogeneously conducting Earth, using Sq as an inducing source field. *Geophys. J. Int.* **151**(3), 913–923 (2002)
- R. Holme, J. Bloxham, Alleviation of the Backus effect in geomagnetic field modelling. *Geophys. Res. Lett.* **22**, 1641–1644 (1995)
- R. Holme, J. Bloxham, The treatment of attitude errors in satellite geomagnetic data. *Phys. Earth Planet. Inter.* **98**, 221–233 (1996)
- R. Holme, M.A. James, H. Lühr, Magnetic field modelling from scalar-only data: Resolving the Backus effect with the equatorial electrojet. *Earth Planets Space* **57**, 1203–1209 (2005)
- G. Hulot, C. Eymin, B. Langlais, M. Manda, N. Olsen, Small-scale structure of the geodynamo inferred from Ørsted and Magsat satellite data. *Nature* **416**, 620–623 (2002)
- G. Hulot, T.J. Sabaka, N. Olsen, The present field, in *Treatise on Geophysics*, vol. 5, ed. by M. Kono (Elsevier, Amsterdam, 2007)
- G. Hulot, N. Olsen, E. Thébault, K. Hemant, Crustal concealing of small-scale core-field secular variation. *Geophys. J. Int.* **177**, 361–366 (2009). doi:[10.1111/j.1365-246X.2009.04119.x](https://doi.org/10.1111/j.1365-246X.2009.04119.x)
- G. Hulot, C. Finlay, C. Constable, N. Olsen, M. Manda, The magnetic field of planet Earth. *Space Sci. Rev.* **152**, 159–222 (2010). doi:[10.1007/s11214-010-9644-0](https://doi.org/10.1007/s11214-010-9644-0)
- A. Jackson, Intense equatorial flux spots on the surface of the Earth's core. *Nature* **424**, 760–763 (2003)
- A. Jackson, C.C. Finlay, Geomagnetic secular variation and its application to the core, in *Treatise on Geophysics*, vol. 5, ed. by M. Kono (Elsevier, Amsterdam, 2007)
- J. Jackson, J. Vette, OGO Program Summary, SP-7601, NASA, 1975
- M.C. Kelley, *The Earth's Ionosphere. Plasma Physics and Electrodynamics*. International Geophysical Series, vol. 96 (Academic Press, Amsterdam, 2009)
- A. Khokhlov, G. Hulot, J. Le Mouél, On the Backus effect—I. *Geophys. J. Int.* **130**, 701–703 (1997)
- A. Khokhlov, G. Hulot, J. Le Mouél, On the Backus effect—II. *Geophys. J. Int.* **137**, 816–820 (1999)
- M.G. Kivelson, C.T. Russell, *Introduction to Space Physics* (Cambridge University Press, Cambridge, 1995)
- J. Korhonen, J. Fairhead, M. Hamoudi, K. Hemant, V. Lesur, M. Manda, S. Maus, M. Purucker, D. Ravat, T. Sazonova, et al., Magnetic Anomaly Map of the World. Map published by Commission for Geological Map of the World, supported by UNESCO, GTK, Helsinki (2007)
- A. Kuvshinov, 3-D global induction in the oceans and solid earth: recent progress in modeling magnetic and electric fields from sources of magnetospheric, ionospheric and oceanic origin. *Surv. Geophys.* **29**(2), 139–186 (2008)
- A.V. Kuvshinov, N. Olsen, A global model of mantle conductivity derived from 5 years of champ, ørsted, and sac-c magnetic data. *Geophys. Res. Lett.* **33**, L18301 (2006). doi:[10.1029/2006GL027083](https://doi.org/10.1029/2006GL027083)
- A.V. Kuvshinov, T.J. Sabaka, N. Olsen, 3-D electromagnetic induction at *Swarm* constellation. Mapping the conductivity anomalies in the mantle. *Earth Planets Space* **58**, 417–427 (2006)
- R.A. Langel, The main field, in *Geomagnetism*, vol. 1, ed. by J.A. Jacobs (Academic Press, London, 1987), pp. 249–512
- R.A. Langel, R.H. Estes, A geomagnetic field spectrum. *Geophys. Res. Lett.* **9**, 250–253 (1982)
- R.A. Langel, R.H. Estes, The near-Earth magnetic field at 1980 determined from MAGSAT data. *J. Geophys. Res.* **90**, 2495–2509 (1985)
- R.A. Langel, W.J. Hinze, *The Magnetic Field of the Earth's Lithosphere: The Satellite Perspective* (Cambridge University Press, Cambridge, 1998)
- R.A. Langel, G. Ousley, J. Berbert, J. Murphy, M. Settle, The MAGSAT mission. *Geophys. Res. Lett.* **9**, 243–245 (1982c)
- R.A. Langel, J.D. Philipps, R.J. Horner, Initial scalar magnetic anomaly map from magsat. *Geophys. Res. Lett.* **9**, 269–272 (1982a)
- R.A. Langel, C.C. Schnetzler, J.D. Philipps, R.J. Horner, Initial vector magnetic anomaly map from magsat. *Geophys. Res. Lett.* **9**, 273–276 (1982b)
- R.A. Langel, T.J. Sabaka, R.T. Baldwin, J.A. Conrad, The near-earth magnetic field from magnetospheric and quiet-day ionospheric sources and how it is modeled. *Phys. Earth Planet. Inter.* **98**, 235–267 (1996)

- F.J. Lowes, Vector errors in spherical harmonic analysis of scalar data. *Geophys. J. R. Astron. Soc.* **42**, 637–651 (1975)
- H. Lühr, S. Maus, Direct observation of the F region dynamo currents and the spatial structure of the EEJ by CHAMP. *Geophys. Res. Lett.* **33** (2006). doi:[10.1029/2006GL028374](https://doi.org/10.1029/2006GL028374)
- H. Lühr, S. Maus, M. Rother, First in-situ observation of night-time F region currents with the CHAMP satellite. *Geophys. Res. Lett.* **29**(10), 127-1 (2002)
- H. Lühr, M. Rother, S. Maus, W. Mai, D. Cooke, The diamagnetic effect of the equatorial appleton anomaly: its characteristics and impact on geomagnetic field modelling. *Geophys. Res. Lett.* **30**(17), 1906 (2003). doi:[10.1029/2003GL017407](https://doi.org/10.1029/2003GL017407)
- H. Maeda, T. Iyemori, T. Araki, T. Kamei, New evidence of a meridional current system in the equatorial ionosphere. *Geophys. Res. Lett.* **9**, 337–340 (1982)
- C. Manoj, A.V. Kuvshinov, S. Maus, H. Lühr, Ocean circulation generated magnetic signals. *Earth Planets Space* **58**, 429–437 (2006)
- S. Maus, CHAMP magnetic mission, in *Encyclopedia of Geomagnetism and Paleomagnetism*, ed. by D. Gubbins, E. Herrero-Bervera (Springer, Heidelberg, 2007a)
- S. Maus, Electromagnetic ocean effects, in *Encyclopedia of Geomagnetism and Paleomagnetism*, ed. by D. Gubbins, E. Herrero-Bervera (Springer, Heidelberg, 2007b)
- S. Maus, H. Lühr, A gravity-driven electric current in the Earth's ionosphere identified in CHAMP satellite magnetic measurements. *Geophys. Res. Lett.* **33**, L02812 (2006). doi:[10.1029/2005GL024436](https://doi.org/10.1029/2005GL024436)
- S. Maus, M. Rother, R. Holme, H. Lühr, N. Olsen, V. Haak, First scalar magnetic anomaly map from CHAMP satellite indicates weak lithospheric field. *Geophys. Res. Lett.* **29**(10), 47-1 (2002)
- S. Maus, F. Yin, H. Lühr, C. Manoj, M. Rother, J. Rauberg, I. Michaelis, C. Stolle, R. Müller, Resolution of direction of oceanic magnetic lineations by the sixth-generation lithospheric magnetic field model from CHAMP satellite magnetic measurements. *Geochem. Geophys. Geosyst.* **9**(7), Q07021 (2008). doi:[10.1029/2008GC001949](https://doi.org/10.1029/2008GC001949)
- S. Maus, U. Barckhausen, H. Berkenbosch, N. Bourmas, J. Brozena, V. Childers, F. Dostaler, J. Fairhead, C. Finn, R. von Frese, et al., EMAG2: A 2-arc min resolution Earth Magnetic Anomaly Grid compiled from satellite, airborne, and marine magnetic measurements. *Geochem. Geophys. Geosyst.* **10**(8), Q08005 (2009)
- J. Merayo, J.L. Jørgensen, M. Blanke, N. Olsen, T. Risbo, F. Primdahl, H. Lühr, GRADSAT: a Danish geomagnetic gradient mission, in *NASA Conference Publication*, vol. 206900 (NASA, Huntsville, 1998), pp. 239–254
- T. Neubert, F. Christiansen, Small-scale, field-aligned currents at the top-side ionosphere. *Geophys. Res. Lett.* **30**(19), 19 (2003). doi:[10.1029/2003GL017808](https://doi.org/10.1029/2003GL017808)
- T. Neubert, M. Manda, G. Hulot, R. von Frese, F. Primdahl, J.L. Joergensen, E. Friis-Christensen, P. Stauning, N. Olsen, T. Risbo, Ørsted satellite captures high-precision geomagnetic field data. *EOS Trans. AGU* **82**(7), 81–88 (2001)
- N. Olsen, Ionospheric F region currents at middle and low latitudes estimated from Magsat data. *J. Geophys. Res.* **102**(A3), 4563–4576 (1997)
- N. Olsen, A model of the geomagnetic field and its secular variation for epoch 2000 estimated from Ørsted data. *Geophys. J. Int.* **149**(2), 454–462 (2002)
- N. Olsen, Ørsted, in *Encyclopedia of Geomagnetism and Paleomagnetism*, ed. by D. Gubbins, E. Herrero-Bervera (Springer, Heidelberg, 2007)
- N. Olsen, S. Kotsiaros, Magnetic satellite missions and data, in *IAGA Special Sopron Book Series*, vol. 5, ed. by B. Hulqvist (Springer, Heidelberg, 2010)
- N. Olsen, R. Holme, G. Hulot, T. Sabaka, T. Neubert, L. Tøffner-Clausen, F. Primdahl, J. Jørgensen, J.M. Léger, D. Barraclough, J. Bloxham, J. Cain, C. Constable, V. Golovkov, A. Jackson, P. Kotzé, B. Langlais, S. Macmillan, M. Manda, J. Merayo, L. Newitt, M. Purucker, T. Risbo, M. Stampe, A. Thomson, C. Voorhies, Ørsted initial field model. *Geophys. Res. Lett.* **27**, 3607–3610 (2000)
- N. Olsen, E. Friis-Christensen, G. Hulot, M. Korte, A.V. Kuvshinov, V. Lesur, H. Lühr, S. Macmillan, M. Manda, S. Maus, M. Purucker, C. Reigber, P. Ritter, M. Rother, T. Sabaka, P. Tarits, A. Thomson, *Swarm—End-to-End mission performance simulator study*, ESA contract No. 17263/03/NL/CB, DSRI Report 1/2004, Danish Space Research Institute, Copenhagen (2004)
- N. Olsen, T.J. Sabaka, L. Gaya-Pique, Study of an improved comprehensive magnetic field inversion analysis for *Swarm*, DNSC Scientific Report 1/2007, Danish National Space Center, Copenhagen, 2007
- N. Olsen, K. Glassmeier, X. Jia, Separation of the magnetic field into external and internal parts. *Space Sci. Rev.* **152**, 135–157 (2010a). doi:[10.1007/s11214-009-9563-0](https://doi.org/10.1007/s11214-009-9563-0)
- N. Olsen, G. Hulot, T.J. Sabaka, Sources of the geomagnetic field and the modern data that enable their investigation, in *Handbook of Geomathematics*, ed. by W. Freeden, Z. Nashed, T. Sonar (Springer, Heidelberg, 2010b)

- V.O. Papitashvili, F. Christiansen, T. Neubert, Field-aligned currents during IMF similar to 0. *Geophys. Res. Lett.* **28**(15), 3055–3058 (2001)
- M.E. Purucker, Magsat, in *Encyclopedia of Geomagnetism and Paleomagnetism*, ed. by D. Gubbins, E. Herrero-Bervera (Springer, Heidelberg, 2007)
- M. Purucker, K. Whaler, Crustal magnetism, in *Treatise on Geophysics*, vol. 5, ed. by M. Kono (Elsevier, Amsterdam, 2007), pp. 195–235
- M. Purucker, B. Langlais, N. Olsen, G. Hulot, M. Manda, The southern edge of cratonic north America: evidence from new satellite magnetometer observations. *Geophys. Res. Lett.* **29**(15), 8000 (2002). doi:[10.1029/2001GL013645](https://doi.org/10.1029/2001GL013645)
- M. Purucker, T. Sabaka, G. Le, J.A. Slavin, R.J. Strangeway, C. Busby, Magnetic field gradients from the ST-5 constellation: improving magnetic and thermal models of the lithosphere. *Geophys. Res. Lett.* **34**(24) (2007). doi:[10.1029/2007GL031739](https://doi.org/10.1029/2007GL031739)
- D. Ravat, R. Langel, M. Purucker, J. Arkani-Hamed, D. Alsdorf, Global vector and scalar Magsat magnetic anomaly maps. *J. Geophys. Res.* **100**(B10), 20111–20136 (1995)
- R.D. Regan, J.C. Cain, W.M. Davis, A global magnetic anomaly map. *J. Geophys. Res.* **80**, 794–802 (1975)
- C. Reigber, H. Lühr, P. Schwintzer, CHAMP mission status. *Adv. Space Res.* **30**, 129–134 (2002)
- P. Ritter, H. Lühr, Curl-**B** technique applied to *Swarm* constellation for determining field-aligned currents. *Earth Planets Space* **58**, 463–476 (2006)
- T.J. Sabaka, R.T. Baldwin, Modeling the Sq magnetic field from POGO and Magsat satellite and contemporaneous hourly observatory data: Phase I (1993)
- T.J. Sabaka, N. Olsen, Enhancing comprehensive inversions using the *Swarm* constellation. *Earth Planets Space* **58**, 371–395 (2006)
- T.J. Sabaka, N. Olsen, R.A. Langel, A comprehensive model of the quiet-time near-Earth magnetic field: Phase 3. *Geophys. J. Int.* **151**, 32–68 (2002)
- T.J. Sabaka, N. Olsen, M.E. Purucker, Extending comprehensive models of the Earth's magnetic field with Ørsted and CHAMP data. *Geophys. J. Int.* **159**, 521–547 (2004). doi:[10.1111/j.1365-246X.2004.02421.x](https://doi.org/10.1111/j.1365-246X.2004.02421.x)
- T.J. Sabaka, G. Hulot, N. Olsen, Mathematical properties relevant to geomagnetic field modelling, in *Handbook of Geomathematics*, ed. by W. Freeden, Z. Nashed, T. Sonar (Springer, Heidelberg, 2010)
- J.A. Slavin, G. Le, R.J. Strangeway, Y. Wang, S.A. Boardsen, M.B. Moldwin, H.E. Spence, Space technology 5 multi-point measurements of near-Earth magnetic fields: initial results. *Geophys. Res. Lett.* **35**(2) (2008). doi:[10.1029/2007GL031728](https://doi.org/10.1029/2007GL031728)
- D.P. Stern, R.A. Langel, G.D. Mead, Backus effect observed by Magsat. *Geophys. Res. Lett.* **7**, 941–944 (1980)
- C. Stolle, H. Lühr, M. Rother, G. Balasis, Magnetic signatures of equatorial spread *F*, as observed by the CHAMP satellite. *J. Geophys. Res.* **111**, A02304 (2006). doi:[10.1029/2005JA011184](https://doi.org/10.1029/2005JA011184)
- B. Tapley, S. Bettadpur, M. Watkins, C. Reigber, The gravity recovery and climate experiment: mission overview and early results. *Geophys. Res. Lett.* **31**(9), L09607 (2004)
- P. Tarits, N. Grammatica, Electromagnetic induction effects by the solar quiet magnetic field at satellite altitude. *Geophys. Res. Lett.* **27**(24), 4009–4012 (2000)
- E. Thebault, K. Hemant, G. Hulot, N. Olsen, On the geographical distribution of induced time-varying crustal magnetic fields. *Geophys. Res. Lett.* **36**, L01307 (2009). doi:[10.1029/2008GL036416](https://doi.org/10.1029/2008GL036416)
- E. Thébault, M. Purucker, K.A. Whaler, B. Langlais, T.J. Sabaka, The magnetic field of the Earth's lithosphere. *Space Sci. Rev.* (2010). doi:[10.1007/s11214-010-9667-6](https://doi.org/10.1007/s11214-010-9667-6)
- L. Tøffner-Clausen, T.J. Sabaka, N. Olsen, End-To-End mission simulation study (E2E+), in *Proceedings of the Second International Swarm Science Meeting* (ESA, Noordwijk, 2010)
- R.H. Tyler, S. Maus, H. Lühr, Satellite observations of magnetic fields due to ocean tidal flow. *Science* **299**, 239–241 (2003)
- P. Ultré-Guérard, M. Hamoudi, G. Hulot, Reducing the Backus effect given some knowledge of the dip-equator. *Geophys. Res. Lett.* **25**(16), 3201–3204 (1998). doi:[10.1029/98GL02211](https://doi.org/10.1029/98GL02211)
- D. Wiese, W. Folkner, R. Nerem, Alternative mission architectures for a gravity recovery satellite mission. *J. Geod.* **83**(6), 569–581 (2009). doi:[10.1007/s00190-008-0274-1](https://doi.org/10.1007/s00190-008-0274-1)